Spindle oscillation in cats: the role of corticothalamic feedback in a thalamically generated rhythm

Diego Contreras and Mircea Steriade*

Laboratoire de Neurophysiologie, Faculté de Médecine, Université Laval, Quebec, Canada

1. Spindles represent an oscillatory activity (7–14 Hz) of the electroencephalogram (EEG) originating in the thalamus and appearing during early stages of sleep. We investigated: (i) the phase relations between thalamic and cortical neurons during this rhythm; (ii) the patterns of spindles under different anaesthetics and their modifications at various levels of the membrane potential (V_m); and (iii) the potentiating role of the corticothalamic feedback in the genesis of spindles. Intra- and extracellular recordings were performed in cats from reticular and dorsal thalamic nuclei, as well as from various cortical areas.

2. In thalamic reticular neurons, spindles were sequences of waves at 7–14 Hz, riding on a prolonged depolarizing plateau and occurring in phase with depth-negative cortical EEG waves. In thalamocortical cells, spindles consisted of inhibitory postsynaptic potentials (IPSPs) in phase with depth-positive cortical EEG waves and occasionally leading to rebound spike bursts. In cortical cells, spindle waves were rhythmic (7–14 Hz) excitatory postsynaptic potentials (EPSPs) that sometimes gave rise to action potentials. Spindles occurred in phase among thalamic reticular, thalamocortical and neocortical neurons.

3. In thalamic reticular neurons, spindle waves and their depolarizing plateaux increased in amplitude with slight cellular hyperpolarization, but at a V_m more negative than −80 or −85 mV they decreased in amplitude. No frequency alterations were observed with these V_m changes.

4. The waxing-and-waning pattern of spontaneous spindles under barbiturate anaesthesia was distinct from the waning pattern under ketamine–xylazine anaesthesia. Under all anaesthetics, spindles had a waning pattern when elicited by cortical stimuli. The amplitude of cortical-evoked spindle waves diminished with the decrease in stimulation intensity.

5. Under urethane or ketamine–xylazine anaesthesia, spindle sequences were grouped by a cortically generated slow oscillation (< 1 Hz) and were preceded by a depth-positive EEG wave that corresponded to a prolonged hyperpolarization in all three investigated (cortical, thalamic reticular, and thalamocortical) cellular types.

6. We propose that the waxing pattern of spindle oscillation is due to a progressive entrainment of units into the oscillation until a maximum number is reached, depending on the background activity in the network. The phase relations between cortical, thalamic reticular and thalamocortical neurons are ascribed to distributed excitatory signals from thalamocortical neurons to both cortical and reticular neurons at each cycle of the oscillation. In turn, cortical neurons provide a powerful drive to potentiate the genesis of thalamic spindles.

Spindle waves appear at a frequency of 7–14 Hz and represent a major rhythm of the electroencephalogram (EEG) that typically occurs during early stages of resting sleep in animals and humans. Spindles survive in the thalamus after bilateral decortication and upper brainstem transection (Morison & Bassett, 1945). In thalamocortical (TC) cells, spindles are built up by cyclic inhibitory postsynaptic potentials (IPSPs), occasionally leading to

* To whom correspondence should be addressed.

rebound spike bursts which are transferred to the cerebral cortex (Andersen & Andersson, 1968; Steriade, Jones & Llinás, 1990).

Two different hypotheses were advanced to explain the origin of spindle-related IPSPs in TC cells. The first one was a model based on intranuclear recurrent inhibition through excitation of local-circuit neurons by collateral axons of TC cells (Andersen & Andersson, 1968). In most dorsal thalamic nuclei, including the ventroposterior (VP) complex where Andersen's experiments were conducted, the axons of TC cells do not give rise to intranuclear recurrent collaterals (Yen & Jones, 1983; Steriade & Deschênes, 1984). The other hypothesis proposed that it is the thalamic reticular (RE) nucleus, consisting of neurons that use γ-aminobutyric acid (GABA) as transmitter, that plays the decisive role in the genesis of rhythmic IPSPs in TC cells (Steriade, Deschênes, Domich & Mulle, 1985). This idea stemmed from experimental data showing the abolition of spindle oscillations in TC neurons disconnected from RE inputs (Steriade *et al.* 1985) and the preservation of spindles within the rostral pole of the RE nucleus isolated from the dorsal thalamus and cortex (Steriade, Domich, Oakson & Deschênes, 1987). That RE neurons impose rhythmic IPSPs onto TC cells was further supported by intracellular recordings showing that, during the IPSPs of TC cells, GABAergic RE neurons discharge prolonged spike barrages within the spindle frequency, superimposed over a depolarizing plateau (Steriade & Deschênes, 1988). It was also demonstrated that, during natural sleep, the short postinhibitory spike bursts that are occasionally fired by TC cells stand in contrast with the discharges of RE neurons throughout spindle sequences (Steriade, Domich & Oakson, 1986). While all these results seemed to justify the claim that RE neurons play a pacemaking role in the production of spindles, it was emphasized that, in the intact brain, any excitatory input may effectively drive the conditional RE pacemaker. Such inputs could include focal hyperpolarizations followed by rebound spike bursts in TC cells that would trigger the RE neuron network which, by virtue of widely distributed thalamic projections, may contribute to the synchronization of the whole thalamus (Steriade *et al.* 1987).

It is now recognized that spindle oscillations depend on both intrinsic properties of thalamic cells and complex network operations in thalamocorticothalamic loops. The Ca^{2+}-dependent low-threshold spike (LTS) crowned by high-frequency Na^{+} action potentials is a basic intrinsic property of TC cells (Llinás & Jahnsen, 1982) which is uncovered by membrane potential (V_m) hyperpolarization during sleep (see Steriade *et al.* 1990). *In vitro* studies revealed the intrinsic properties and ionic conductances of singly oscillating RE cells (Avanzini, De Curtis, Panzica & Spreafico, 1989; Huguenard & Prince, 1992, 1994; Bal & McCormick, 1993) and supported the notion of a thalamic pacemaker. However, without network operations, spindles would not be observed synchronously in many thalamic foci and widespread cortical areas (Andersen & Andersson, 1968; Steriade *et al.* 1990). Moreover, an oscillation at < 1 Hz, generated within the cerebral cortex (Steriade, Nuñez & Amzica, 1993*b*,*c*) and reflected in RE and TC cells (Steriade, Contreras, Curró Dossi & Nuñez, 1993*a*), contributes to the grouping and synchronization of sleep rhythms, including spindles, within slowly recurring wave-sequences (Contreras & Steriade, 1995).

Although spindles are generated in the thalamus even in the absence of the cerebral cortex, cortical inputs potentiate spindles as this oscillation is elicited by corticothalamic volleys, even by stimulating the contralateral cortex to avoid the antidromic invasion of TC axons (Steriade, Wyzinski & Apostol, 1972). Intracellular recordings showed that corticothalamic stimuli are much more efficient than prethalamic volleys in eliciting spindles in TC neurons (see Fig. 1.3 in Steriade *et al.* 1990).

The present work was undertaken to study the patterns of spontaneous and evoked spindles under different anaesthetics, the dependency of spindles upon the intrinsic electrophysiological properties of RE and TC cells, and the role of corticothalamic volleys in the elicitation and synchronization of spindles. We used simultaneous intra- and extracellular recordings of cortical, RE and TC neurons belonging to sensory, motor and association systems. Throughout this article we define 'spindle' as a sequence of rhythmic waves at 7–14 Hz and we use the term 'depolarizing plateau' to designate the prolonged depolarization over which spindle waves are riding in RE cells recorded *in vivo*.

METHODS

Experiments were conducted on adult cats anaesthetized with pentobarbitone (35 mg kg^{-1}, I.P.), ketamine–xylazine (10–15 and 2–3 mg kg^{-1}, respectively, I.M.) or urethane (1·8 g kg^{-1}, I.P.). In addition, all pressure points and tissues to be incised were infiltrated with lidocaine. The animals were paralysed with gallamine triethiodide only after the EEG showed the typical patterns of deep general anaesthesia. The animals were artificially ventilated to an end-tidal CO_2 of 3·5–3·7%. The heart beat was continuously monitored and showed rates (between 90 and 110 min^{-1}) that assessed the depth of anaesthesia. Body temperature was maintained at 37–39 °C. Saline glucose was supplemented as a fluid therapy, 1–2 times during the experiment. The EEG was continuously recorded throughout the experiments. To monitor the depth of anaesthesia, we maintained a constant picture of high-amplitude and low-frequency EEG waves. Lower doses of the same anaesthetic were administered (2–3 times during an experiment) at the slightest changes in EEG patterns, i.e. a tendency towards increased frequency and decreased amplitudes of EEG waves. Experiments lasted for 8–10 h.

Intracellular recordings were performed with glass micropipettes filled with a solution of 3 M potassium acetate and DC resistances of 35–45 MΩ. (i) Cortical intracellular recordings were performed after resection of the bone and dura. Mineral oil was used to prevent desiccation. The pipettes for intracellular recordings in the cortex were placed in the vicinity of the coaxial EEG recording

electrodes (see below). (ii) For thalamic intracellular recordings, the cortex and white matter over the recorded thalamic territory were removed by suction. Micropipettes were then lowered through the head of the caudate nucleus in order to reach the rostrolateral sector of the RE nucleus and the ventrolateral (VL) nucleus. The stability of intracellular recordings was improved by performing a bilateral pneumothorax, as well as by the drainage of the cisterna magna, hip suspension, and by filling the holes made for recording with a solution of 4% agar. A high-impedance amplifier (bandpass of 0–5 kHz) with active bridge circuitry was used to record and inject current into the cells. Extracellular recordings were done by means of tungsten electrodes with resistances of 1–5 MΩ. Signals were recorded on an eight-channel tape with bandpass of 0–9 kHz and thereafter were digitized at 20 kHz for off-line computer analysis.

The gross EEG was recorded monopolarly by means of a screw inserted in the bone. The focal EEG was recorded by means of coaxial electrodes with the tip placed in deep cortical layers and the ring over the pial surface. The EEG recording electrodes were inserted in the lateral part of the precruciate motor cortex (area 4), the postcruciate somatosensory cortex (areas 3b, 1 and 2), and the rostral suprasylvian association cortex (area 5). The depth was adjusted to obtain an inverse polarity of the thalamic-evoked potential. In all monopolar recordings the indifferent electrode was placed in the neck muscles. Besides, the electrothalamogram (EThG) was bipolarly recorded through the same electrodes as used for stimulation.

Stimulating coaxial electrodes were stereotaxically placed in the motor VL thalamic nucleus and the brachium conjunctivum (BC), the somatosensory VP thalamic nuclear complex and the dorsal column nuclei (DCN), or the association lateroposterior (LP) thalamic nucleus, according to the system under study. Cortical stimulation was performed by means of the coaxial electrodes used for EEG recording.

At the end of experiments the cats were given a lethal dose of pentobarbitone.

RESULTS

Data base and neuronal identification

The results are based on recordings from 208 cortical neurons, 233 RE neurons, and 129 TC neurons. Cortical cells ($n = 143$ intra, $n = 65$ extra) were recorded from the motor, primary somatosensory, and association suprasylvian cortices. RE cells ($n = 70$ intra, $n = 163$ extra) were recorded from the rostral pole, rostrolateral (peri-VL), and lateral (peri-VP and peri-LP) sectors of the nucleus. TC neurons ($n = 26$ intra, $n = 103$ extra) were recorded from the VL, VP and LP nuclei. The intracellularly recorded neurons that were used for the data base and analyses had stable V_m, more negative than −60 mV for cortical cells or more negative than −55 mV for thalamic cells, and overshooting action potentials.

(i) Cortical cells were located in layers II to VI. Motor cortical neurons were identified by an excitatory postsynaptic potential (EPSP) evoked by VL and BC stimulation. Cells from the somatosensory cortex responded to stimulation of the appropriate body region. They displayed EPSPs in response to stimulation of VP and DCN (see Fig. 2*B*). (ii) Neurons from the RE nucleus were identified by their prolonged spike bursts and accelerando–decelerando bursting pattern during spontaneous oscillatory activity (Domich, Oakson & Steriade, 1986; see Fig. 5*Ad*) and burst responses to stimulation of cortical and thalamic input sources. (iii) TC cells from the VL nucleus were identified by antidromic invasion and EPSPs in response to motor cortex stimulation, followed by a sequence of IPSPs at the spindling frequency, occasionally giving rise to rebound spike bursts. TC cells recorded extracellularly were identified by their short, high-frequency spike bursts with a decelerando pattern in response to motor cortex stimulation (VL cells) or to DCN or receptive field stimulation (VP cells).

Cortical cells

Under barbiturate anaesthesia, cortical cells spontaneously displayed oscillations at 7–14 Hz, grouped in spindle sequences that recurred periodically with a slow rhythm of 0·1–0·3 Hz. Spindling in cortical cells was characterized by rhythmic EPSPs (occasionally leading to action potentials) which increased in amplitude towards the middle of the spindle sequence and thereafter decreased in amplitude (Figs 1*A* and 2*Aa*). The cellular oscillatory activity was reflected in the EEG, most commonly as depth-negative (surface-positive) waves. In some instances, the EEG waves were more complex, with a mixture of positive and negative components that changed their shape during the spindle sequence (see Fig. 2*Aa*).

During spindles, cortical cells that were simultaneously recorded within a distance of 1–1·5 mm exhibited synchronized oscillatory activity ($n = 15$). Figure 1 depicts two intracellularly recorded neurons at depths of 0·5 and 0·7 mm, simultaneously with the surface and depth EEG in their vicinity, an extracellularly recorded cell population from VP thalamus and focal waves recorded through the same thalamic microelectrode. The six traces shown in *A* were averaged around the negative peaks of depth EEG waves (Fig. 1*B*) in order to assess the phase relation during the oscillatory activity. The averaged oscillation shows that the depth-negative waves of the cortical EEG corresponded to depolarizations of both cortical cells as well as to firing of TC cells (peri-event histogram, bottom, Fig. 1*B*) and negative field potentials in the focal EThG recorded from the VP nucleus. The depolarizations of cortical neurons started before the peak negativity of depth EEG waves and were related to the field thalamic waves.

Another example of synchronous spindling in simultaneous intracellular recordings from cortical cells is shown in Fig. 2*Aa* depicting two neurons recorded from the suprasylvian area 5, together with the surface and depth EEG in their vicinity and the field potentials from the corresponding thalamic LP nucleus. In cortical intracellular recordings, the spontaneous spindles were expressed as subthreshold EPSPs with a characteristic waxing-and-waning pattern, namely, a progressive increase in the amplitude of the EPSPs (associated with a similar increase

in cortical and thalamic field potentials towards the middle of the spindle sequence), followed by a progressive decrease in the amplitudes of oscillatory events. Upon thalamic LP stimulation (Fig. 2*Ab*), the evoked spindle sequence showed a waning pattern, with the EPSPs and EEG waves showing only a progressive decrease in amplitude.

Similar phase relations and prevalent waning pattern of the evoked spindling were observed in the series of intracellular responses of two simultaneuously recorded SI neurons to DCN stimulation, depicted in Fig. 2*B* together with a cell from the corresponding region in the thalamic VP nuclear complex. The two SI cells, separated by about 1·3 mm, displayed DCN-evoked spindle sequences in which the first three waves were in phase. The following EPSPs within the spindle sequence were of smaller amplitude and were not synchronized. The peristimulus histogram of VP cell population firing (bottom trace of Fig. 2*B*) shows two clear oscillatory peaks, followed by irregular discharges. The fact that the second peak was delayed by 20 ms after the EPSPs of cortical cells suggests that this VP neuron lagged slightly the main thalamic population impinging upon the recorded cortical cells. These data suggest that the waning pattern of cortical spindling is due to a process of desynchronization of the TC input.

Spindle oscillations under ketamine–xylazine anaesthesia (Fig. 3) were grouped by a slow rhythm (< 1 Hz), characterized by long-lasting positive waves in the depth EEG, followed by sharp negative deflections leading to a spindle oscillation. By contrast to the waxing-and-waning pattern of spindles under barbiturate anaesthesia,

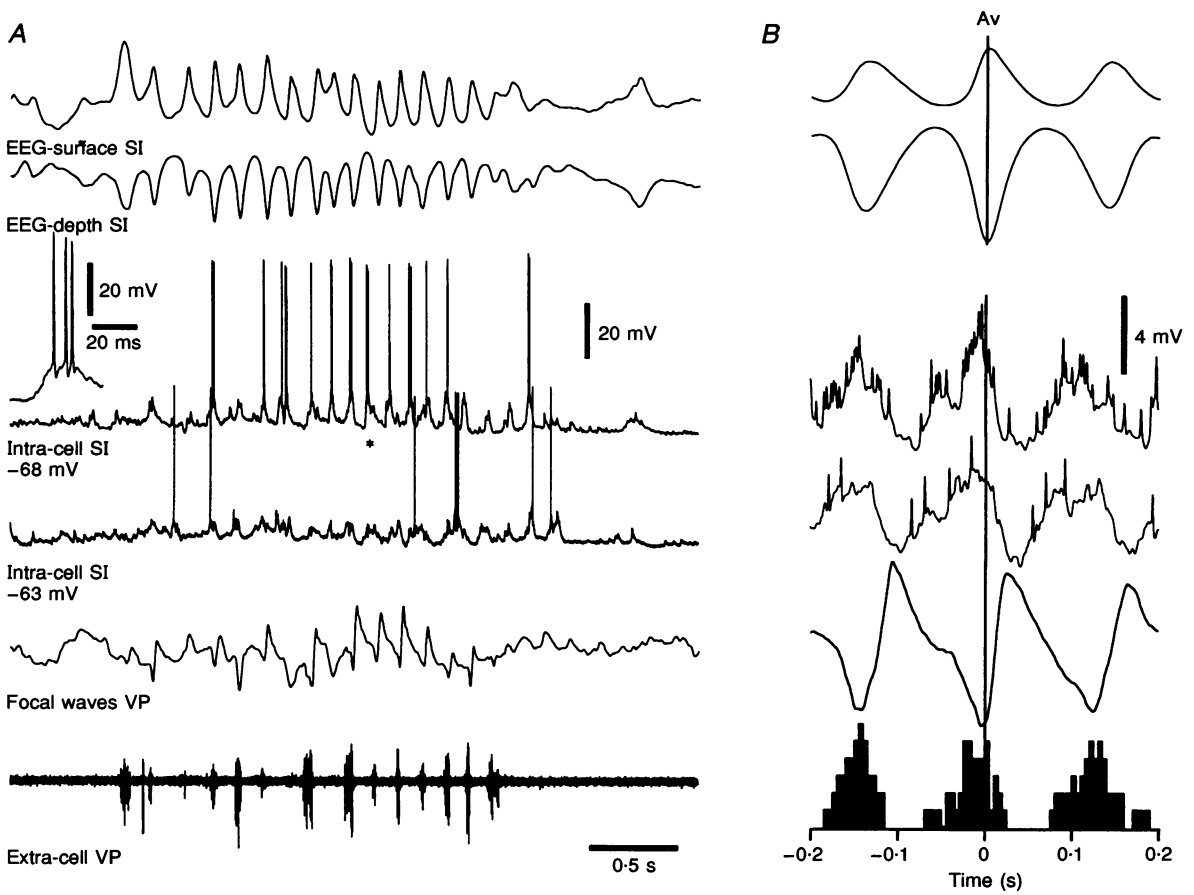

Figure 1. Waxing-and-waning spindle oscillations occur in phase in related thalamic and cortical territories

Barbiturate anaesthesia. Two cells from the primary somatosensory cortex (SI), separated by about 1 mm, were impaled and simultaneously recorded together with the EEG from the surface (EEG-surface) and depth (EEG-depth) in the cortical vicinity. In addition, a neuronal population was extracellularly recorded from the VP nucleus; the two bottom traces illustrate the focal waves (field potentials) through the same microelectrode that was used to record action potentials. *A*, spontaneous waxing-and-waning spindle sequence at around 8 Hz, consisting of EEG depth-negative deflections that reversed polarity at the surface. Both cells displayed EPSPs in phase with the EEG deflections. *expanded in inset. *B*, average (Av, $n = 15$) of traces shown in *A* centred on the depth-negative peak of EEG potentials. In this and following figures, V_m is indicated; field potentials are averaged whenever single cell activity is averaged; and the polarity of EEG is the same as for intracellular recordings (positivity up).

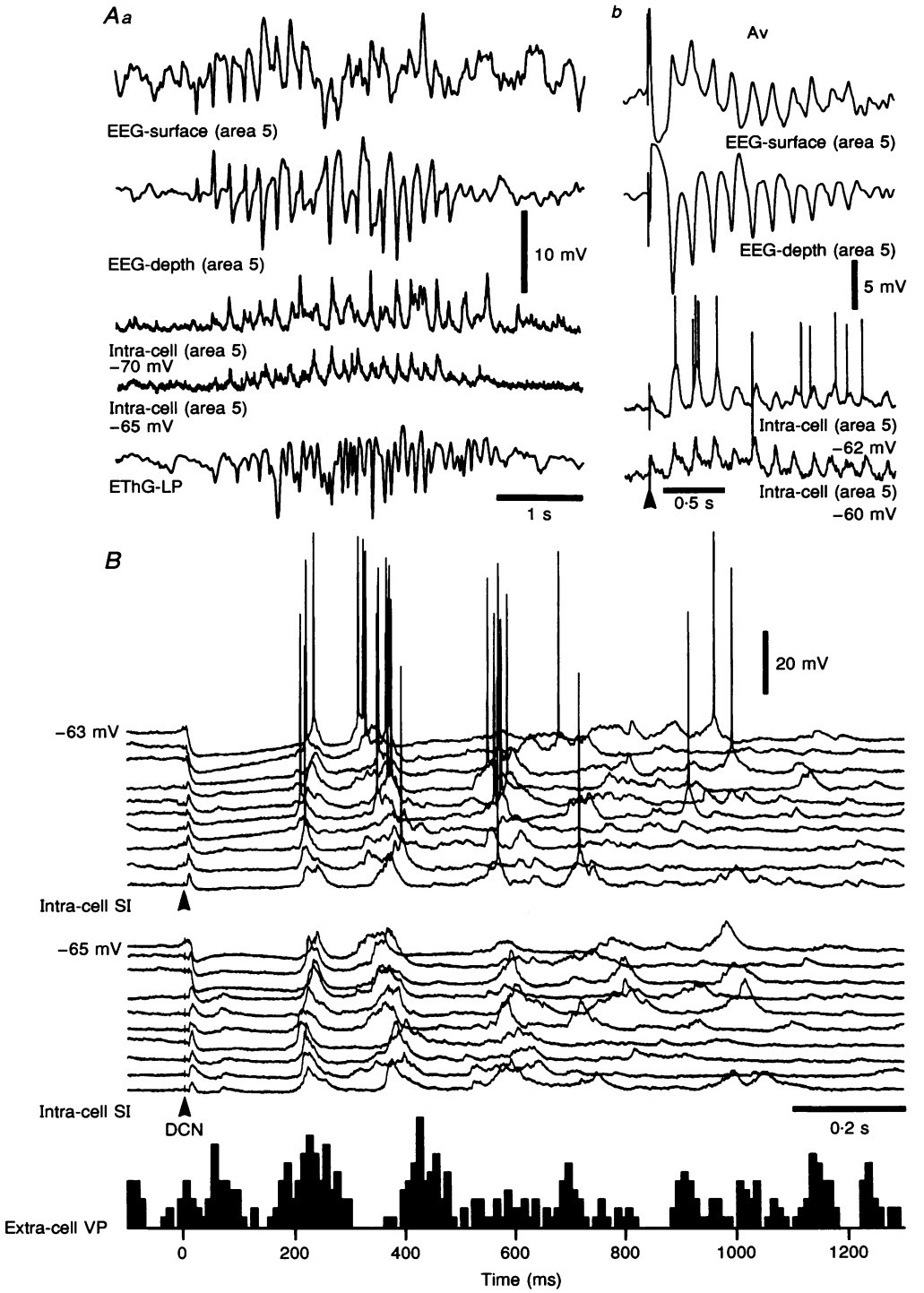

Figure 2. Spindle oscillations preferentially display a waning pattern when elicited by synchronous stimuli to central pathways

Barbiturate anaesthesia. *A*, two cells were simultaneously recorded intracellularly from area 5 (1·5 mm apart). In *Aa*, they displayed spontaneously occurring, synchronized spindle oscillations, together with the surface and depth EEG from area 5 in the vicinity of cells and with the EThG from the LP nucleus. In *Ab*, average (Av, $n = 15$) of LP-evoked responses in the same two cortical cells and EEG activities. *B*, intracellular activities of two SI cortical cells, simultaneously recorded with extracellular activities from a thalamic VP nucleus. The two cortical cells responded to DCN stimulus with a spindle sequence that displayed a waning pattern. In both intracellular recordings, the 10 traces were displaced vertically for clarity and represent the responses of two cells (at a constant V_m) to DCN shocks of constant parameters. The bottom trace represents the peristimulus histogram from the thalamic VP cells' population and similarly shows prevalent waning of the spindle sequence in response to DCN stimuli.

spontaneous spindle sequences under ketamine–xylazine were mostly waning. Consequently, the spontaneous spindling was similar to that evoked by cortical or thalamic stimulation under the same anaesthetic (Fig. 3).

The intracellular counterpart of the depth-positive EEG waves in cortical neurons was a reduced or abolished synaptic activity associated with a 4–7 mV hyperpolarization that lasted for 0·3–0·6 s, in parallel with the duration of those EEG waves (Fig. 4*A*). An extracellular, simultaneous recording of a neuronal population from the thalamic VP nucleus showed a period of neuronal silence, in close time relation to the depth-positive EEG waves and the hyperpolarization of cortical neurons (Contreras & Steriade, 1995). To determine the phase relation during spontaneous spindling, an average was computed around the negative peaks of depth EEG potentials (Fig. 4*B*). The oscillatory behaviour shows a one-to-one, in phase relation, between the depth EEG, the intracellular cortical recording and the extracellular recording of the thalamic VP population. The same aspect resulted from the analysis of evoked spindles (Fig. 4*C*).

Thalamic reticular cells

Under ketamine–xylazine anaesthesia, the spontaneous spindle oscillations of RE cells were characterized by a waning pattern (Fig. 5*Aa–c*), similar to that observed in the cortical EEG under the same anaesthesia (see above). The depolarizing plateau, over which the rhythmic spike bursts of RE cells occurred, reached its maximum amplitude from the onset of a spindle sequence and its duration was closely related to that of the spindle sequence in the cortical EEG. Spindles were preceded by a hyperpolarization of RE cells that corresponded to the depth-positive EEG cortical wave. The RE-cell's spike bursts occurred in phase with the negative peaks of the depth-cortical EEG activity (Fig. 5). Due to the depolarizing plateau of RE cells during spindle oscillations, the burst firing led to tonic discharge towards the end of spindle sequences (see panel *Ab* in Fig. 5).

The phase relation between EEG and RE-intracellular activities was also observed for the evoked spindling, with either cortical or dorsal thalamic stimulation ($n = 22$). In the RE neuron shown in Fig. 5*Ba*, a stimulus applied to the motor cortex induced a high-frequency spike burst superimposed upon an EPSP, that was followed by a slight hyperpolarization corresponding to a depth-positive (surface-negative) EEG wave. The cell oscillated almost one-to-one with the EEG. This relation was emphasized by averaging multiple responses (Fig. 5*Bb*).

The phase relations between RE cells and cortical activities during spindle oscillations were further investigated by performing intracellular recordings from motor cortex, simultaneously with extracellular recordings of RE cells from the rostrolateral (peri-VL) sector ($n = 16$). Figure 6 depicts such a couple. The cortical cell oscillated

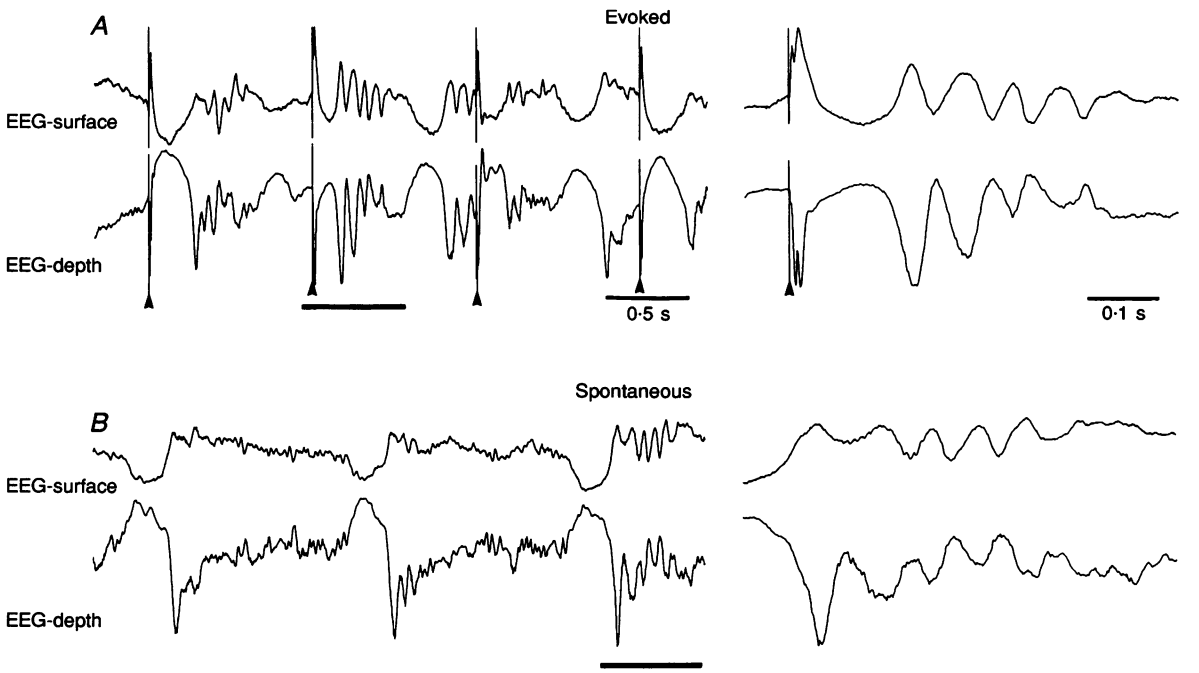

Figure 3. Under ketamine–xylazine anaesthesia, both evoked and spontaneously occurring EEG spindle sequences display a waning pattern

Recordings from precruciate part of area 4. *A*, series of responses to white matter stimulation (Evoked), recorded through a coaxial electrode with its ring on the surface and the tip at a depth of 0·7 mm. A detail of the second response (horizontal bar) is expanded on the right. *B*, spontaneous activity recorded by the same electrode (Spontaneous). The last spindle sequence is expanded on the right.

spontaneously at the spindling frequency, in phase with depth-negative cortical EEG waves as well as the spike bursts of the thalamic RE neuron. The averaged activities of the cortical cell and EEG from ten spindle sequences are illustrated together with the peri-event histogram of the RE neuron, all centred around the first negative peak of EEG waves.

Cortical-evoked spindle oscillations in RE cells were decreased in amplitude and duration by decreasing the intensity of the applied stimuli ($n = 28$). Figure 7 shows that, by decreasing the amount of current used to stimulate the cortex, (i) the evoked spindle sequence started earlier (because the preceding hyperpolarization was shorter); (ii) the spindle sequence was gradually shorter in duration and exhibited fewer oscillatory cycles; (iii) the amplitudes of individual waves were smaller; and (iv) the amplitude of the depolarizing plateau decreased progressively. At low intensities of stimulation (bottom trace in Fig. 7*A* and *B*), it was possible to evoke a single EPSP or an EPSP followed by a small hyperpolarization that were not followed by oscillatory behaviour. The changes in the intensity of stimulation did not alter the frequency of the evoked oscillatory episode. The early responses to cortical stimuli of varying intensities are expanded on the right hand side and indicate that they also decreased gradually, in parallel with the reduction of stimulating current applied to cortex.

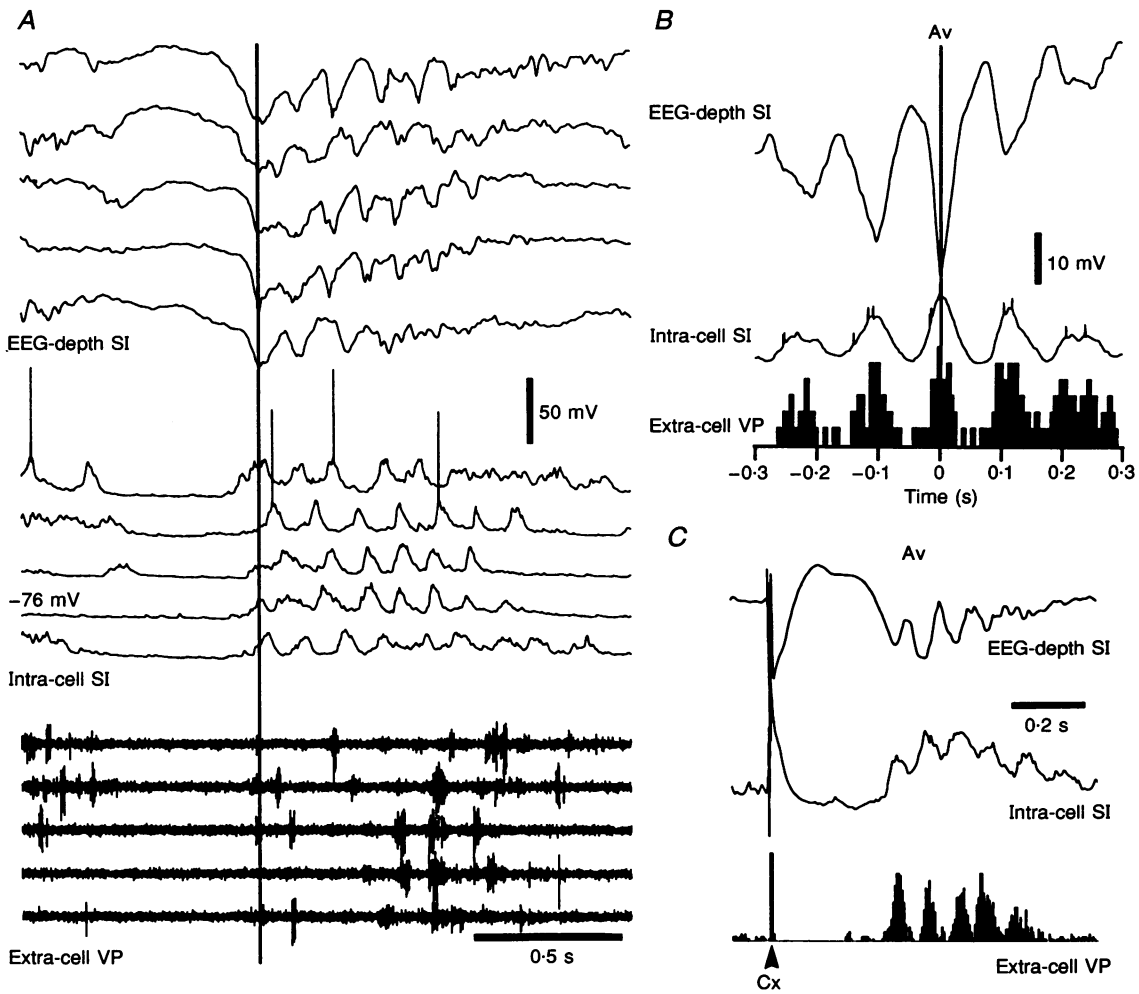

Figure 4. Spindle sequences during ketamine–xylazine anaesthesia occur in phase among cortical and thalamic neurons

A, spontaneous spindle sequences recorded simultaneously by an EEG electrode placed in the depth of SI cortex, an intracellular pipette from an SI cell in the vicinity of the EEG lead, and an extracellular electrode picking up a population of TC cells from the thalamic VP nucleus. Five spontaneous spindle sequences were aligned on the first negative peak of each sequence and displaced vertically. *B*, two top traces are the average (Av, $n = 32$) of the EEG and the cell represented in *A*. Bottom trace is the peri-event histogram from VP cells, all centred on the EEG negative peaks. *C*, same neurons and the corresponding EEG displayed a similar phase relation upon stimulation of SI cortex (arrowhead, Cx) by a coaxial electrode in the proximity of the intracellular recording.

Spindle oscillations in RE cells were altered not only by modifying the corticothalamic input, but also by changing the V_m of the cell with current injection ($n = 17$). The rostrolateral RE neuron illustrated in Fig. 8 was intracellularly recorded under barbiturate anaesthesia. The neuron displayed spontaneous spindle oscillations (S) that typically consisted of waxing-and-waning depolarizing waves over a depolarizing plateau. The RE cell also responded with spindle oscillations to motor cortical stimulation (on the right, stimuli indicated by arrowheads). Changes in the V_m by current injection influenced both the individual waves during a spontaneous spindle sequence

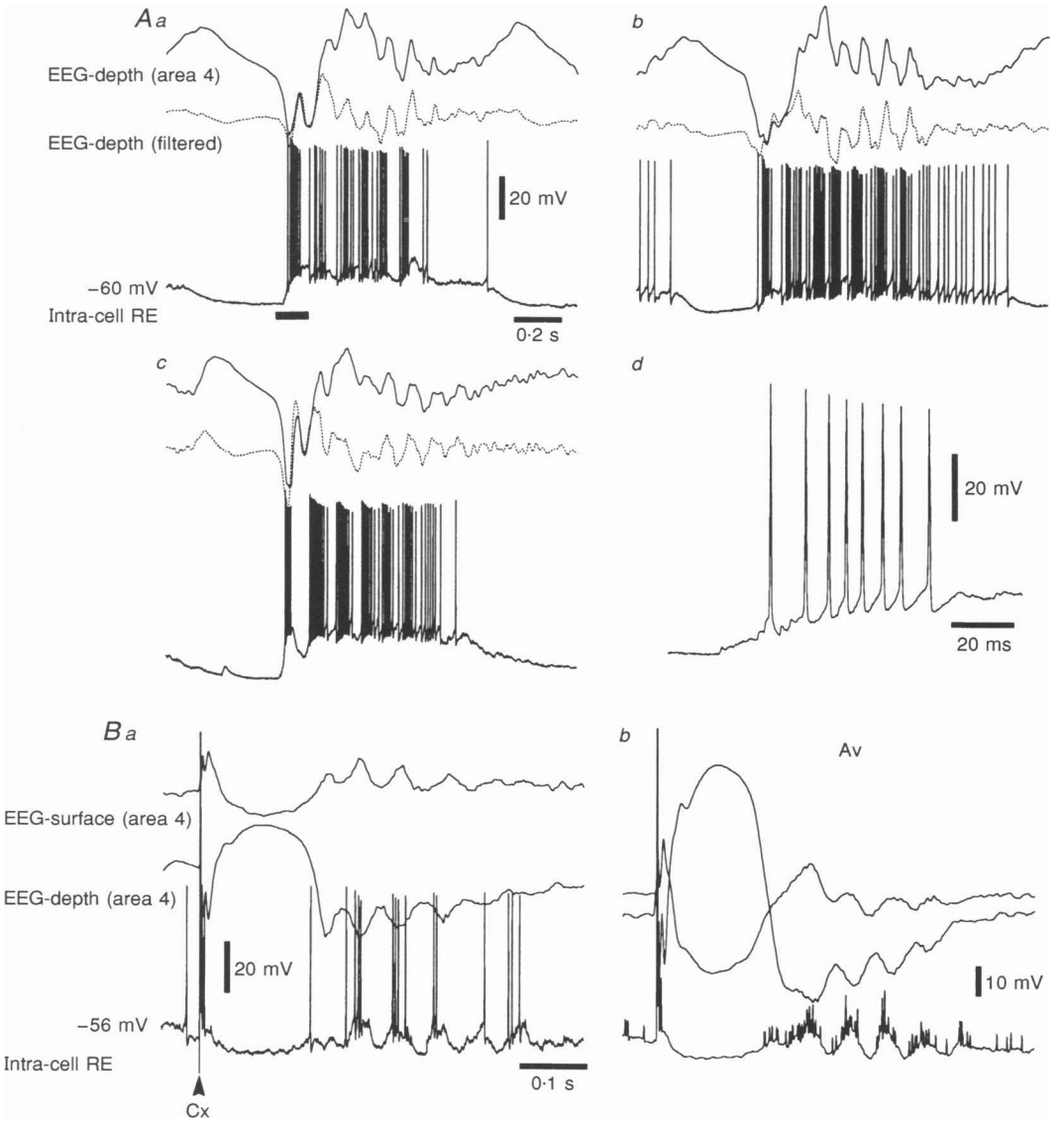

Figure 5. Phase relations between spindling in RE cells and cortical EEG

Ketamine–xylazine anaesthesia. *A* and *B*, intracellular recordings of two RE cells from the rostrolateral sector, simultaneously with the EEG from cortical motor area 4. *A*, the filtering of EEG waves between 0·3 and 100 Hz (dotted trace), enhanced the spindling oscillation and diminished the slow components of the EEG. *Aa–c*, 3 different spontaneous spindle sequences. The oscillatory behaviour within the frequency range of spindles was preceded by a cellular hyperpolarization that corresponded to a depth-positive EEG wave. RE cell's spike bursts corresponded very closely, in a one-to-one fashion, to the depth-negative EEG cortical waves that characterize spindling. In *Ad*, expanded first burst of the oscillation shown in *Aa* (horizontal bar). It shows an accelerando–decelerando pattern and a long duration (around 60 ms), both features being characteristic for spike bursts of RE cells. *B*, a single response of rostrolateral RE cell to cortex stimulation is shown for a relatively depolarized membrane potential (−56 mV), together with the EEG from the surface and depth of the motor cortex. The cell oscillated in phase with the depth-negative EEG waves that reversed polarity at the surface. *Bb* illustrates an average (Av) of 15 consecutive responses of the same cell to cortical stimuli of constant parameters.

and the associated depolarizing plateau (see dotted line in panel *C*, at −84 mV) that increased in amplitude with hyperpolarization and decreased with depolarization. It is also clear that neither the frequency of the oscillation nor its duration changed with the polarization of the cell. This behaviour was the same for the spontaneous and evoked activities. Note that the evoked activity had a depolarizing plateau of a slightly higher amplitude than the spontaneous spindle sequences (especially visible in *B*), suggestive of the role played by cortical synaptic inputs in sustaining the plateau.

Further hyperpolarization, however, had the effect of decreasing the amplitude of both spindle waves and depolarizing plateau (Fig. 9). In this figure, the two different (*A* and *B*) neurons recorded under urethane anaesthesia responded to shocks applied to the motor cortex with spindle waves riding on a depolarizing plateau that increased in amplitude with hyperpolarization, with a maximum amplitude reached between −70 and −75 mV. Upon further hyperpolarization to V_m levels more negative than −80 mV, the spindles diminished in amplitude in both cells (compare third and bottom traces in *B*, baseline indicated by dots) and were subthreshold for triggering an LTS. The cell depicted in *B* was also recorded at a relatively depolarized V_m (−54 mV) at which level the spindling oscillation was followed by a sustained, tonic discharge at a rate of 70–80 Hz, compared with about 30 Hz prior to the evoked spindle.

To asses the effect of cortical input on the degree of synchronization between RE cells during spindling, pairs of closely located neurons were recorded extracellularly, mostly from the rostrolateral sector of the nucleus ($n = 10$) and the peri-VP region ($n = 8$). The two RE cells (RE 1 and RE 2) recorded from the rostrolateral sector (Fig. 10) showed spontaneous burst firing with rather weak synchrony within the frequency range of spindles, as indicated by the discrete peaks at 100 ms in the detail of the crosscorrelogram of spontaneous activity (bar and arrow). The stimulation of the motor cortex (arrowheads in the upper trace) induced stronger spindling oscillation that was synchronous among the two cells. This is further shown by plotting the peristimulus histograms of both cells against each other in the joint peristimulus histogram (JPSH). The timing between the firing of the two cells can be followed by the clouds representing the intersection of spike occurrence in both cells; dots located on the diagonal line represent coincident firing. The projection of the clouds to a line perpendicular to the diagonal line forms the

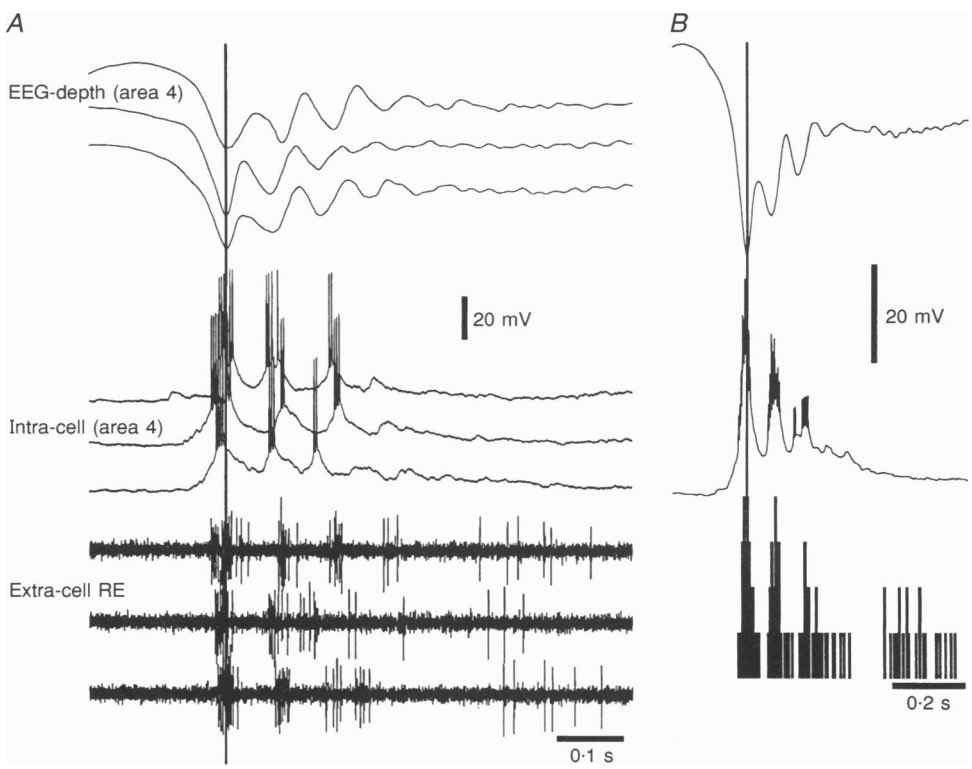

Figure 6. Cortical and RE neurons oscillate in phase during spindling

Ketamine–xylazine anaesthesia. A cortical neuron was recorded intracellularly from the motor cortex, simultaneously with a rostrolateral RE cell as well as the EEG from the depth of area 4. *A*, the 3 traces show spontaneous spindle sequences, aligned by the first EEG negative peak and displaced vertically for clarity. *B*, by using the same alignment point, an average calculated from 10 spontaneous spindle sequences and the peri-event histogram (bin = 5 ms) for the RE cell.

crosscorrelogram depicted on the right, demonstrating rhythmic coincidence of firing at 10 Hz.

Thalamocortical cells

A long series of studies have established that the spindle sequences of TC cells are characterized by a series of IPSPs at 7–14 Hz, occasionally giving rise to rebound spike bursts (see introduction).

Under barbiturate anaesthesia, the rhythmic IPSPs increased in amplitude with the progression of the spindle sequence, reaching a maximum at the mid-sequence, and they decreased in amplitude towards the end of the oscillation (not shown; see Steriade & Deschênes, 1984, 1988).

Under ketamine–xylazine anaesthesia, spindles had an almost exclusive waning pattern (similar to the results from recordings of cortical and thalamic RE neurons reported above), with the maximum hyperpolarization of TC cells being reached from the first IPSPs. Thus, the spindle sequence showed an only-depolarizing trend: successive IPSPs occurred at progressively more depolarized levels (Fig. 11*Ac* and *f*) and spike bursts tended to be progressively smaller (Fig. 11*Ad* and *e*).

Spontaneous spindle oscillations in TC cells were preceded by a hyperpolarization that corresponded to a depth-positive EEG wave (Fig. 11*Aa–c*). The depth-negative EEG waves corresponded with depolarizations in TC cells that eventually reached the threshold for rebound spike bursts.

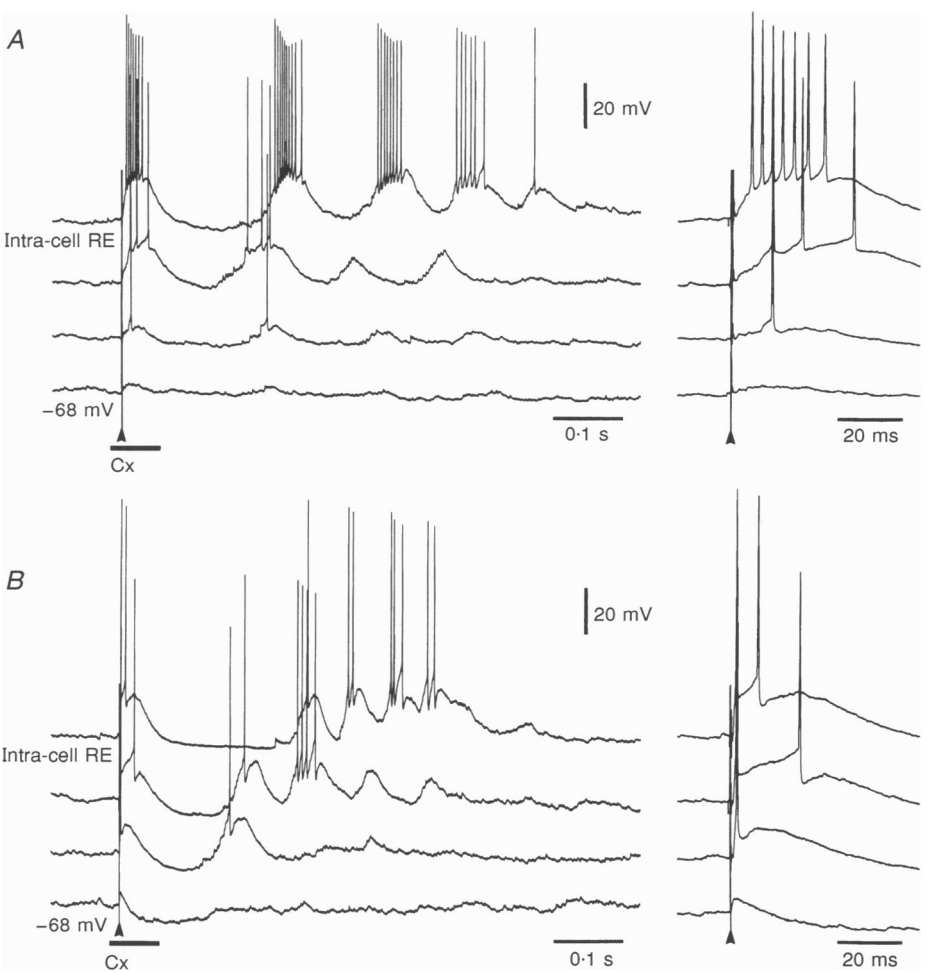

Figure 7. The duration and amplitude of cortical-evoked spindle oscillations are dependent on the intensity of stimulation

A and *B*, two different rostrolateral RE cells, both from experiments under urethane anaesthesia. Responses to motor cortical stimulation. Sweeps from top to bottom depict responses at a constant V_m to stimuli of decreasing intensities. RE neurons responded to stimulation with a characteristic sequence of events, consisting of an EPSP giving rise to a spike burst or one action potential, followed by a hyperpolarization and a spindle sequence (note, in the upper sweep of both cells, the clear depolarizing plateau at the highest intensity of stimulation). On the right, an expanded detail of the early response to each stimulus (part marked by horizontal bar below the bottom trace in both *A* and *B*).

The spontaneous spindle sequences in the VL neuron depicted in Fig. 11 were aligned on the sharp depth-negative EEG deflections that characterize the slow oscillation and initiate spindle sequences under ketamine–xylazine anaesthesia. The EEG traces were filtered between 0·3 and 100 Hz to eliminate the slow components (< 1 Hz) and to enhance the spindle oscillation (dotted lines in *Aa–c*). A sequence of events similar to

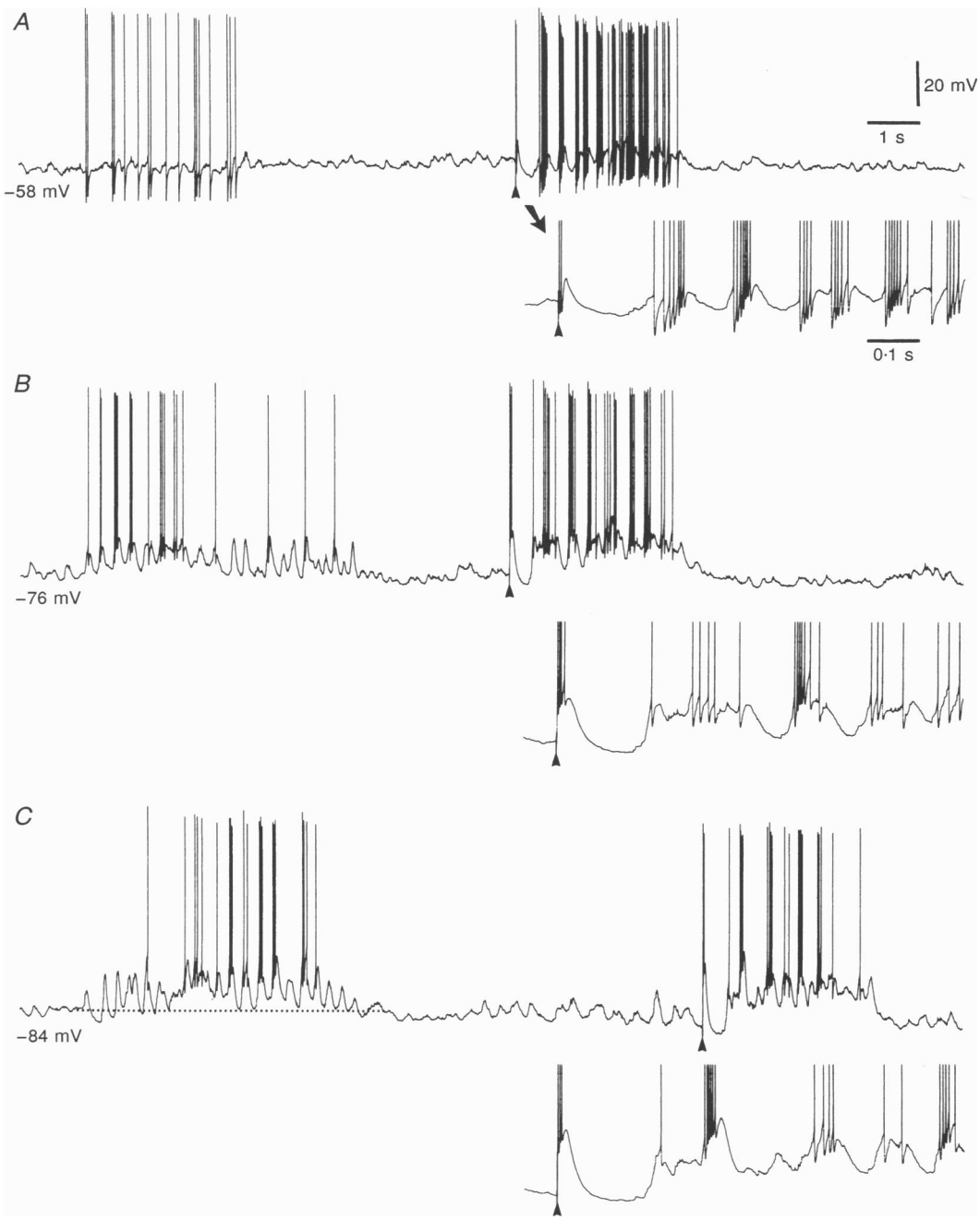

Figure 8. Voltage dependency of spindle oscillations in RE neuron under barbiturate anaesthesia

Intracellular recording of RE neuron from the rostrolateral sector. Three panels are depicted (*A–C*), at different V_m values. The cell was depolarized (−58 mV, in *A*) or hyperpolarized (−84 mV, *C*) from the resting level (−76 mV, *B*) by means of DC current injection through the micropipette (in *B*, no current). The cell displayed spontaneous spindle oscillations (on the left in each trace, S in the upper trace) and spindles evoked by cortical stimulation (on the right in each trace, arrowhead). Expanded details of the beginning of evoked spindles are depicted below on the right (arrow in *A*).

spontaneous spindles was observed when spindling was evoked by cortical or thalamic stimulation. Stimuli of identical parameters were applied to the cortex and successive cellular responses were superimposed (Fig. 11*B*). Evoked spindle sequences were initiated after a cellular hyperpolarization that corresponded with a depth-positive EEG wave and were predominantly waning. Spike bursts tended to occur at intervals very close to the depth-negative sharp EEG waves and they could be terminated by IPSPs. This is indicated by the superposition in Fig. 11*Bb* in which LTSs at later intervals in the oscillation and with less action potentials had longer durations.

Spindles were also synchronized between the two hemispheres (Fig. 12). A cell from the thalamic VL nucleus was recorded together with the surface EEG from the contralateral motor cortex. The cell displayed spontaneous spindle oscillations, five of which are displayed in Fig. 12 aligned on the surface-positive EEG peaks. The spindle sequences were preceded by a long-lasting hyperpolarization and were characterized by successive IPSPs,

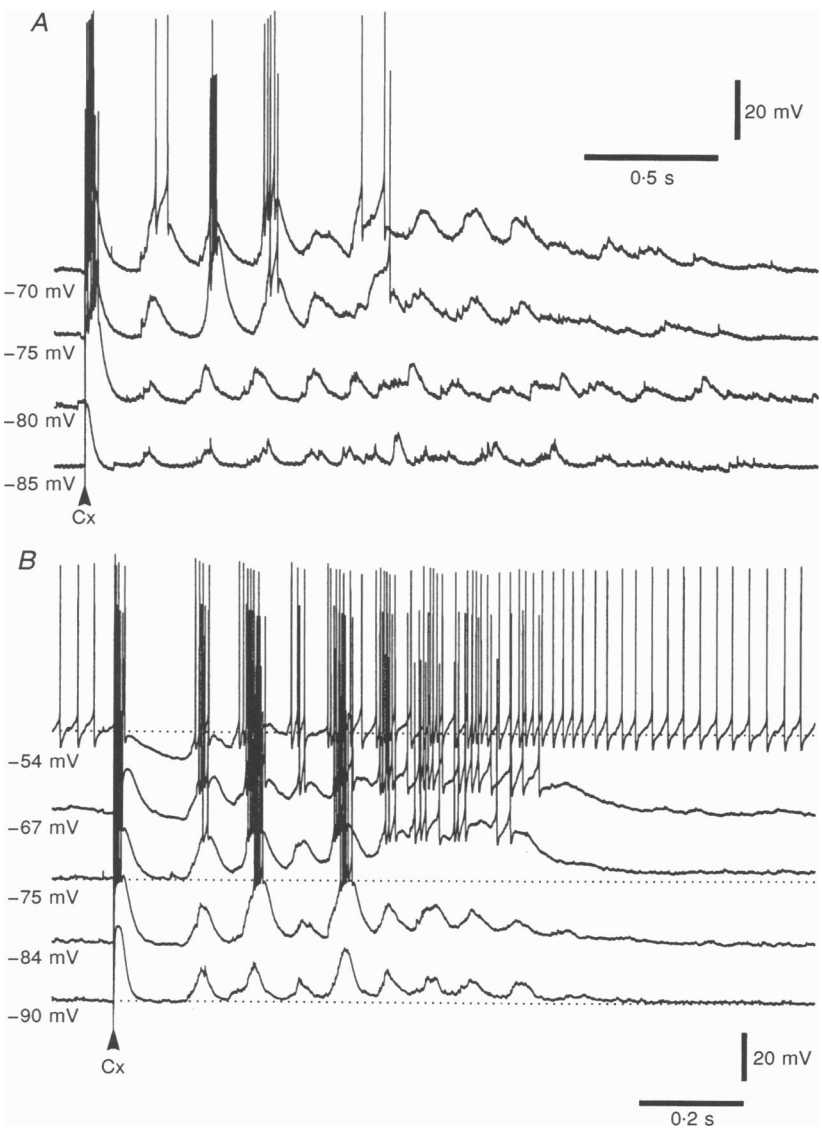

Figure 9. Voltage dependency of spindle oscillations in RE neurons under urethane anaesthesia
A and *B*, 2 neurons from the rostrolateral sector of the RE nucleus. In both cases V_m was hyperpolarized by means of DC current injection while stimulating the cortex with constant parameters. The cells responded with an EPSP triggering a spike burst that was followed by a hyperpolarization and, thereafter, a spindle sequence. In *B*, dotted lines in the first, third and last sweeps tentatively indicate the resting level from which the depolarizing plateau developed. From a depolarized level (−54 mV) to a hyperpolarized V_m (−75 mV) there was a significant increase in the amplitude of both the individual waves that constitute the spindle sequence as well as the depolarizing plateau. Further hyperpolarization progressively decreased the size of both individual waves and depolarizing plateaux.

sometimes leading to rebound spike bursts. The beginning of the oscillation corresponded to a surface-positive EEG peak. Although a jitter in the burst firing can be seen around the positive peak of the EEG (see inset on the right), the temporal coincidence was striking considering the EEG as a gross recording from the contralateral cortex. The components of the spindle oscillation could not be resolved in the EEG as this arises from a large cortical territory. The presence of EEG fast frequencies is probably accounted for by multiples of the spindling frequency due to the convergence of different oscillating spots with small displacements of phase.

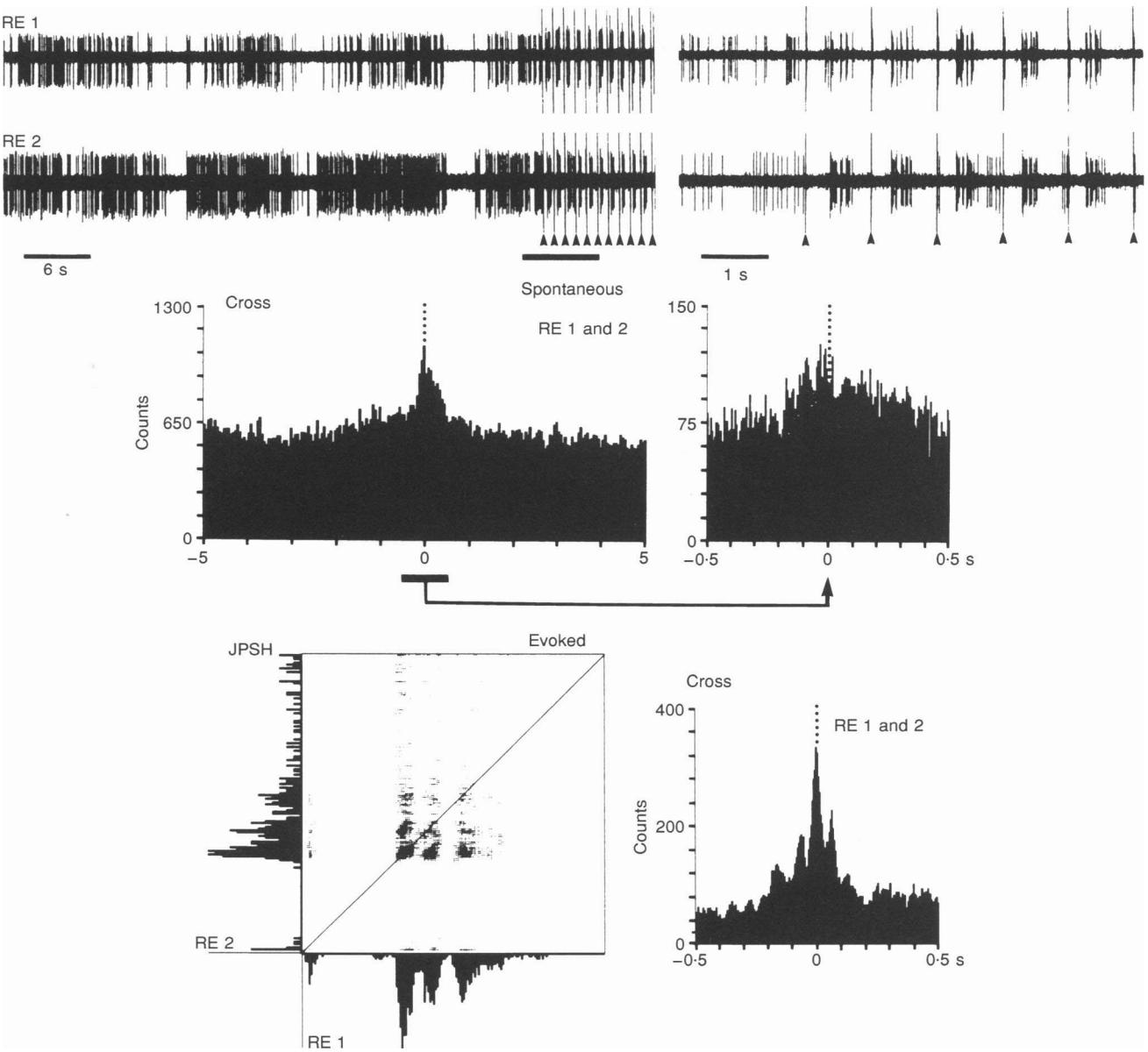

Figure 10. RE cells oscillate in phase during spindling evoked by cortical stimulation

Ketamine–xylazine anaesthesia. Two RE cells from the rostrolateral sector (RE 1 and RE 2, top traces) were recorded simultaneously. Before cortical stimuli, their spontaneous activities displayed a weak tendency to synchronous spindle oscillations (middle panel; the detail indicated by arrow shows discrete peaks at intervals of 100 ms). Cortical shocks (top traces, arrowheads) enhanced the synchronization of spindling activity among the 2 cells, as shown by the joint peristimulus histogram (JPSH; bottom panel), in which the activities of two cells are plotted against each other. The coincident points generate clouds in the plot that fall at the diagonal line for spikes arriving at coincident times. Three cycles of the oscillation elicited by the cortex occurred in phase among the two cells. The averaged crosscorrelogram (Cross) is represented on the right with peaks at 100 ms indicating synchonization within the spindling frequency.

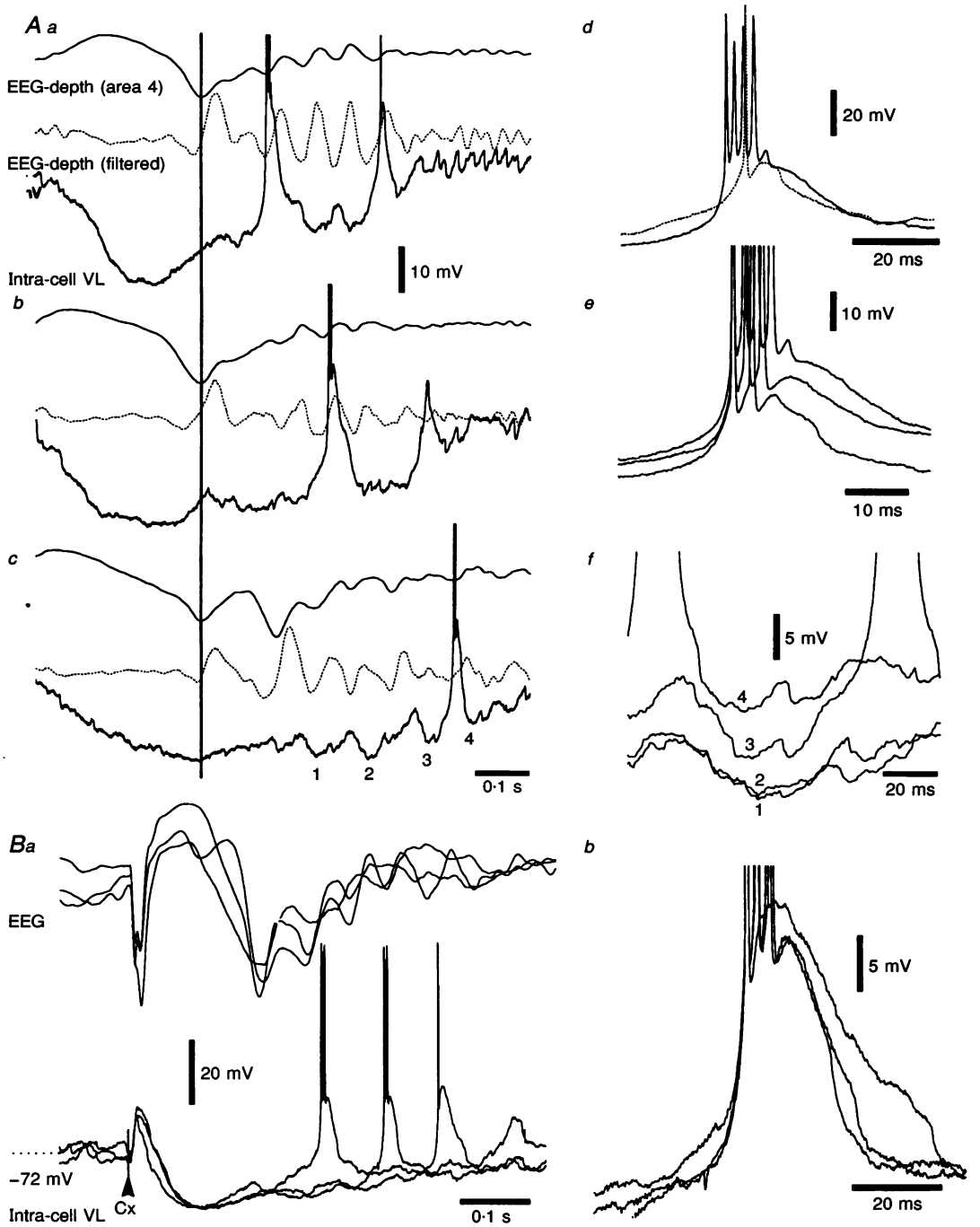

Figure 11. Relations between TC cells and EEG waves during spindle oscillations in corresponding thalamic and cortical territories

A TC cell was intracellularly recorded from the VL nucleus under ketamine–xylazine anaesthesia together with the EEG from the depth of the motor area 4. *Aa–c* are 3 spontaneous spindle sequences (spikes truncated). The middle traces (dotted) represent the depth EEG traces filtered between 0·3 and 100 Hz to enhance spindling. *Ad* shows an expanded detail of two rebound bursts fired by the cell during the sequence depicted in *Aa* (the second and smaller is depicted with a dotted line). *Ae* shows LTSs and Na^+-mediated spike bursts from the spontaneous spindle sequences shown in *Aa* and *b*, occurring progressively closer to the end of the sequences, being progressively smaller in amplitude, and giving rise to smaller numbers of action potentials. Four IPSPs, occurring at progressively more depolarized levels during the spindle sequence depicted in *Ac*, are indicated with the letters 1–4 and superimposed in *Af*. The same relations were observed during spindle sequences evoked by cortical stimulation. *B* shows 3 different responses to cortical stimulation (Cx, arrowhead) from the same cell depicted in *A*. Spike bursts during the oscillation were preceded by depolarization coincident with the EEG negative waves. *Bb* is a detail of the spike bursts depicted in *Ba*.

The TC cells that were slightly depolarized at rest (between −55 and −58 mV) remained silent during spontaneous spindle oscillations ($n = 21$). In Fig. 13*A* the IPSPs characterizing the spindling were in phase with depth-positive EEG waves but, following the depth-negative sharp EEG deflections, no spike burst was fired during the whole spindle sequence. That this could be due to the range of V_m within which the cell oscillated is shown by another cell, depicted in Fig. 13*B*, that responded to cortical stimulation with spindle oscillations which did not give rise to spike bursts at rest (−65 mV) or at depolarized membrane potentials (−55 mV); however, when the cell was hyperpolarized with current (−70 mV), it fired rebound bursts at the release of IPSPs.

To determine the role of input strength in the triggering of spindles, the efficacy of thalamic and prethalamic stimulation was compared in TC cells with stimuli applied to the dorsal thalamus itself and to prethalamic stimuli ($n = 5$). In Fig. 14 a VL cell responded to electrical stimulation of the same nucleus, about 1 mm posteromedial to the cell, with a robust 10 Hz spindle oscillation. The same neuron showed a less ample and much shorter EPSP followed by a biphasic IPSP sequence and a spike burst to stimulation of cerebellothalamic axons, but no sign of spindle oscillatory activity. The other four tested cells displayed a similar behaviour. These results are consistent with previous data showing that, at least in the cerebello–thalamo–cortical system, prethalamic stimuli are

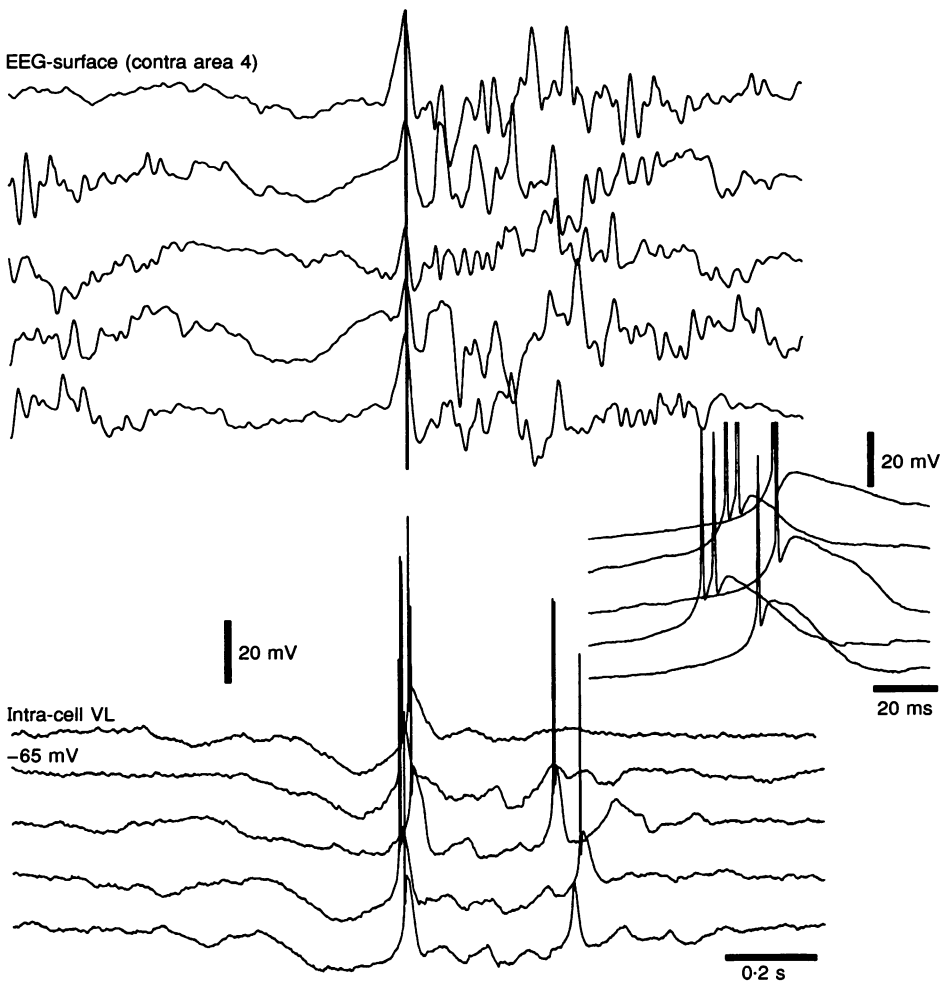

Figure 12. Spindle sequences may occur simultaneously within the two hemispheres

Urethane anaesthesia. A thalamocortical VL cell was intracellularly recorded together with the EEG from the contralateral motor area 4 (contra area 4; screw placed on the bone). Five spontaneous spindle sequences were aligned to the peak positivities of the surface EEG and displaced vertically for clarity. The TC cell was at −65 mV (without current). Spindle sequences were preceded by hyperpolarization that lasted for about 0·2 s. The beginning of the spindle sequence was marked by a positive wave in the contralateral EEG and a rebound spike burst in the VL cell. Despite the fact that the EEG was recorded from the contralateral hemisphere, a striking synchrony between the cell's first burst and the EEG positive wave can be seen in the inset on the right, where a jitter of less than 30 ms appeared when aligning the cellular activity to the surface-positive peak in the EEG.

much less efficient in eliciting spindling (see Introduction and Steriade *et al.* 1972, 1990).

DISCUSSION

Our results show that (i) thalamic and cortical neurons oscillate in phase during spindles; (ii) the waxing-and-waning pattern characterizes the spontaneous oscillation under barbiturate anaesthesia, whereas waning waves appear under ketamine–xylazine anaesthesia as well as when spindling is evoked by synchronous stimuli to the cerebral cortex; (iii) the patterns of spindle-related potentials in RE and TC neurons vary with fluctuations in their V_m; and (iv) corticothalamic volleys potentiate the genesis of spindles.

Phase relations among thalamic and cortical cells during spindling

We assessed the phase relations by comparing the intracellular components of spindles with a common reference, that is, the surface and/or depth EEG potentials recorded from anatomically related cortical fields. The choice of motor, somatosensory and association anterior suprasylvian areas was due to the prevalence of spindles in those cortical regions. In essence, all three investigated cellular classes (cortical, RE and TC neurons) were depolarized during the depth-negative (surface-positive) EEG waves characterizing spindling. RE neurons fired spike bursts with virtually every cycle of the oscillation, while TC and cortical cells discharged irregularly, skipping some spindle cycles, and the participation of their firing in spindling

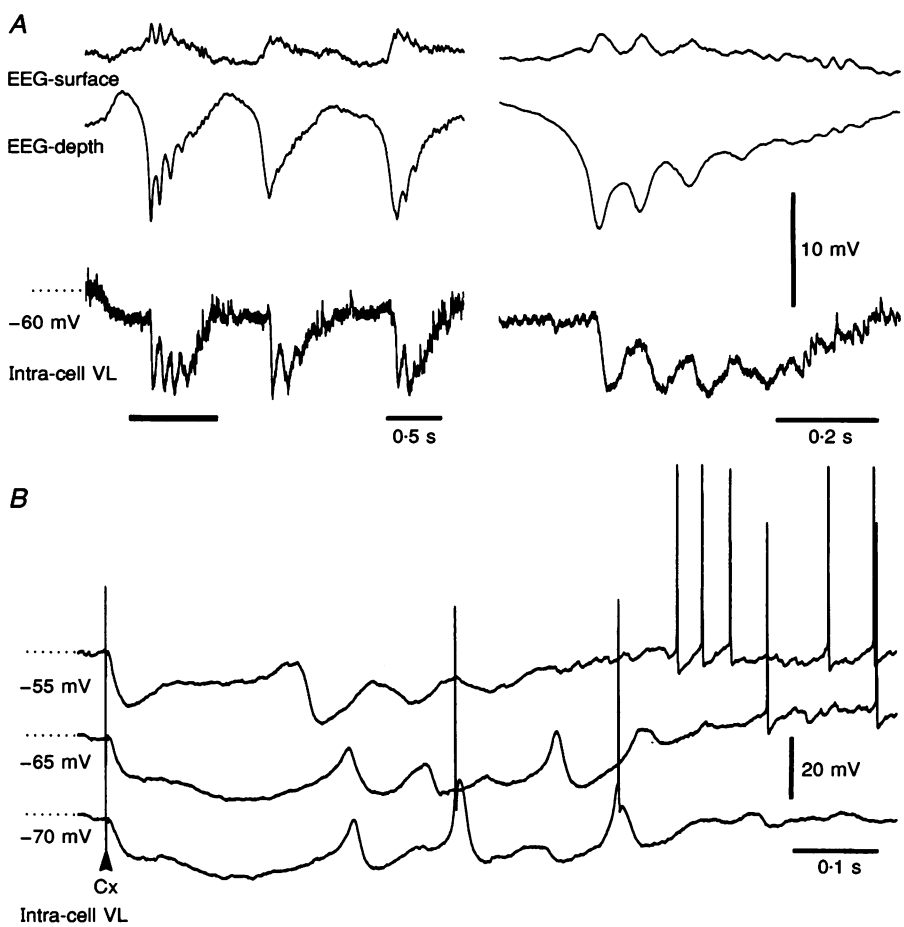

Figure 13. Some TC cells remain silent during spindle oscillations

Ketamine–xylazine anaesthesia. *A*, a TC cell from the VL nucleus, recorded simultaneously with the EEG from the surface and depth of area 4. Slow rhythm at 0·8 Hz, with spindle sequences clearly visible in some cycles. The spindle sequences were reflected in the TC cell as cyclic hyperpolarizations at 10 Hz, but the cell did not fire a single rebound burst. A detail of the first spindle sequence on the left (bar) is shown on the right, where a clear relation is shown between EEG waves and TC-cell's IPSPs. *B*, spindle sequences were evoked by cortical stimulation (arrowhead) while displacing the V_m by DC current injection. At rest (−65 mV) and depolarized levels (−55 mV) IPSPs characterizing the spindle sequence did not reach the V_m range for eliciting a rebound burst. When the cell was hyperpolarized (−70 mV) two rebound bursts were fired by the cell during the spindle oscillation. Note the non-linear behaviour of the second (presumably $GABA_B$ mediated) IPSP evoked by the cortical shock.

Diego Contreras and Mircea Steriade

Journal of Physiology **490**, 159–179 (1996)

On page 175, *the labelling in Figure* 14 *should read*:

Intra-cell VL *and not Intra-cell* (*area 4*).

The legend is correct.

critically depended upon their V_m. It is, however, known from multi-unit recordings within dorsal thalamic nuclei projecting to cortical suprasylvian areas that *every* cycle of focal thalamic spindles is reliably associated with the high-frequency spike bursts of one, another, or all TC neurons (see Fig. 6.8. in Steriade *et al.* 1990). We interpret the phase relations assumed by thalamic and cortical cells during spindling as resulting from the distribution of TC rebound spike bursts onto both RE and cortical neurons at various cycles of the oscillation, with the implication that, *in vivo*, the cortical feedback projections to the thalamus would potentiate the generation of spindles. This assumption is corroborated by the powerful effect of cortical volleys in the elicitation of spindles (see below).

Waxing-and-waning of spindles

Waxing depends on a progressive recruitment and synchronization of thalamic and cortical cells (see also Andersen & Andersson, 1968). This is based on the progressive increase in the amplitude of synaptic potentials in RE, TC and cortical cells during the first part of a spindle sequence, suggesting an increase in the amount of converging inputs onto individual neurons. The increase in synaptic inputs is reflected by the increasing amplitudes of field potentials in the thalamus and cortex (Figs 1 and 2). For a cell to be entrained into spindling, the correct timing of inputs at spindle frequency should dominate the cell's behaviour against the background activity. Thus, in a network with low activity level, such as under barbiturate

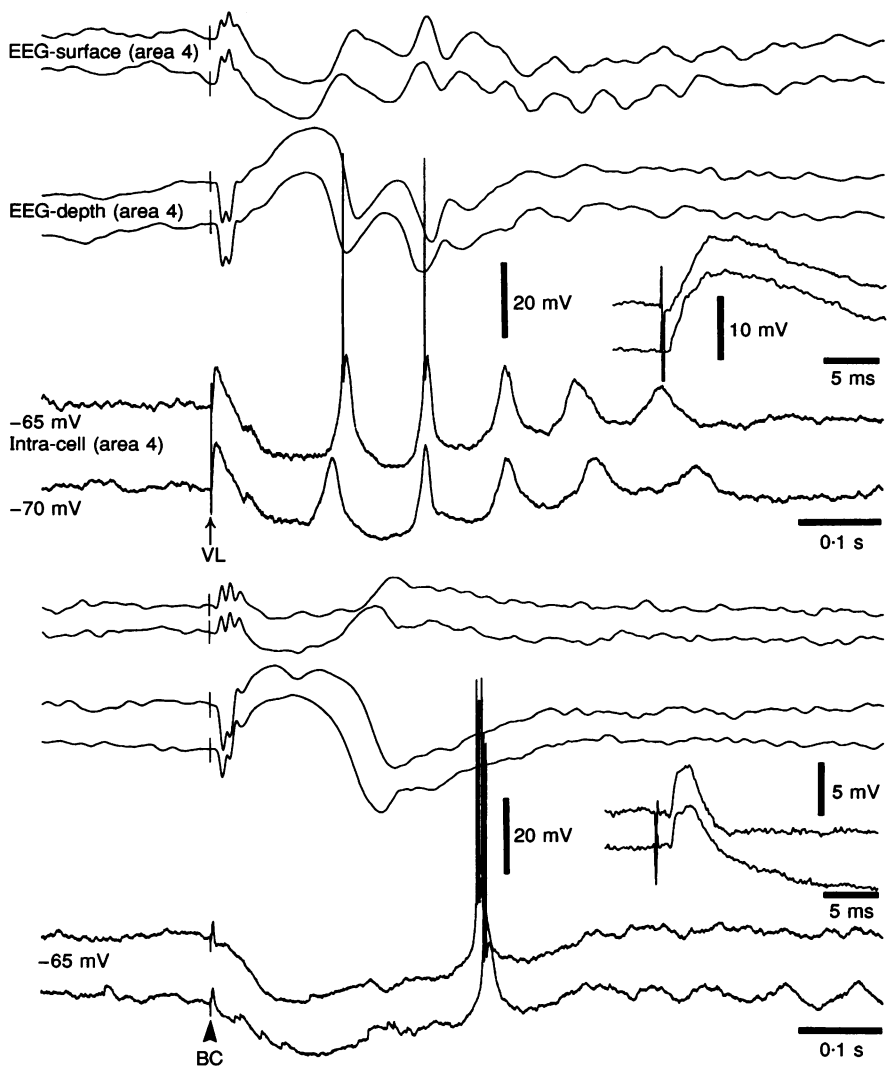

Figure 14. Spindle oscillations depend on the strength of the incoming signals

Ketamine–xylazine anaesthesia. A cell from the VL nucleus was intracellularly recorded together with the EEG from the depth and surface of cortical area 4. The system responded with robust spindling to stimulation of the VL nucleus (posteromedial to the recorded neuron). Responses at rest (−65 mV) and under current (−70 mV) are shown with their respective EEGs. A detail of the early EPSP is shown in the inset on the right. Responses to BC stimulation (arrowhead) did not elicit spindling; the two stimuli were applied at rest (−65 mV). A detail of the early EPSP is depicted on the right.

anaesthesia, the threshold for spindle generation is low, with the consequence that synchronous inputs, initially triggering spike bursts in a relatively small number of thalamic neurons, would eventually lead to a full-blown spindle sequence. It is conceivable that, in a thalamic slice with an even lower background activity, a burst of a single thalamic cell may trigger a whole spindle sequence in the related network. On the contrary, when the thalamic and cortical background activities are high, as is the case under ketamine–xylazine anaesthesia, the threshold of spindle generation is higher, but once a critical neuronal mass is set into the oscillatory mode, there is little further entrainment of cells and the waxing process is unlikely. Spontaneous spindle sequences are observed in those cases in which high synchronization is achieved from the very onset of the oscillation, thus giving rise to preferentially waning spindles. The slow oscillation (< 1 Hz), with its sharp depth-negative component (Fig. 3) reflecting the synchronous excitation of a considerable number of cortical neurons (Contreras & Steriade, 1995), represents a favourable condition for triggering a waning spindle sequence in the pacemaking RE cells and in their TC targets, with a shorter duration than that observed under barbiturate anaesthesia (see Figs 6 and 12, compared to Figs 1 and 2).

The above comments also apply to data from thalamic slices in which succinimide-induced small changes in the probability of burst firing in thalamic cells caused an important reduction in intrathalamic rhythmicity (Huguenard & Prince, 1994). This implies that slight or seemingly negligible alterations in the proportion of thalamic neurons participating in the organization of network activity may be critical for the development of the oscillation. We propose that the background noise in a spontaneously active network, as *in vivo*, plays the role of diminishing the probability of spike bursts in thalamic cells, thus increasing the requirements for converging inputs in order to effectively trigger spindle oscillations. In the same vein, we think that the long-lasting hyperpolarizations, generating widespread neuronal silence, create favourable conditions for generation of synchronized spindling (Contreras & Steriade, 1995).

Although the barbiturate-induced spindling is waxing-and-waning, cortical stimulation gives rise to mostly waning spindles under the same anaesthetic condition (Fig. 2*A*). This leads us to the conclusion that synchronous stimuli entrain, right from the start, a great number of neurons participating in a spindle sequence, which would explain the absence of the waxing process. Evoked spindles occur following a long-lasting hyperpolarization triggered by the cortical stimulus in TC cells. The cellular hyperpolarization also occurs simultaneously in cortical, RE and TC cells, and is reflected as a prolonged depth-positive EEG wave (Contreras & Steriade, 1995). The spontaneously occurring spindling under ketamine–xylazine anaesthesia is mostly waning and preceded by a hyperpolarization having the same characteristics as the evoked one (see Figs 5, 7 and 11). In both cortical and thalamic cells, prolonged hyperpolarizations have been shown to be produced by $GABA_{A,B}$-mediated IPSPs (Connors, Malenka & Silva, 1988; Crunelli, Haby, Jassik-Gerschenfeld, Leresche & Pirchio, 1988). Although the spontaneous long-lasting hyperpolarization of the slow oscillation under ketamine–xylazine anaesthesia is not mainly due to the activation of GABAergic receptors (Contreras & Steriade, 1995), the same principle seems to be valid, i.e. prolonged hyperpolarizations, either spontaneous or stimulus elicited, are effective in setting the scene for widespread synchronization in thalamocortical networks. The synchronizing process includes the appearance of spindle oscillations which follow the sharp depth-negative cortical deflection characteristic of the slow oscillation.

The waning of the oscillations may require, besides the desynchronization of the network (Andersen & Andersson, 1968), the intervention of cellular intrinsic properties capable of diminishing cells' probability of firing spike bursts. Otherwise, the oscillation would be self-sustained and generalized, as is the case with the development from sleep rhythms to epileptic patterns (Avoli, Gloor, Kostopoulos & Gotman, 1983; Steriade & Amzica, 1994; Steriade & Contreras, 1995). The slow inward rectifier I_h, present in TC cells (McCormick & Pape, 1990), may play such a role (Bal, von Krosigk & McCormick, 1995*a*) by depolarizing the cells and bringing them into the range of LTS inactivation. Thus, with the progressive dropout of neurons generating spike bursts, converging inputs onto network elements become smaller and the oscillation fades. This possibility is supported by the present results showing that IPSPs related to the waning of spindles occur on a background of progressive depolarization (Fig. 11*A*). That cellular desynchronization contributes to the waning of spindles (see Andersen & Andersson, 1968) is suggested by the fact that, during waning, EPSPs in cortical neurons become not only smaller but also scattered (Fig. 2*B*).

Voltage dependency of spindling in thalamic reticular and thalamocortical cells

Spindle sequences in RE cells recorded *in vivo* are characterized by prolonged spike bursts at 7–14 Hz, with an acceleration followed by a deceleration of intraburst frequency (Domich *et al.* 1986; Steriade *et al.* 1986). The long duration and peculiar burst patterns of RE cells are due to a special type of I_t (Huguenard & Prince, 1992), probably located in the dendrites. The spindle-related discharges of RE neurons are superimposed on a depolarizing plateau (Mulle, Madariaga & Deschênes, 1986; Contreras, Curró Dossi & Steriade, 1993). The present data show that the depolarizing plateau of RE neuronal discharges throughout a spindle sequence is increased with

hyperpolarization down to −75 or −80 mV and then decreases in amplitude with further hyperpolarization, together with the individual spindle waves (Figs 8 and 9).

A series of arguments point to the participation of synaptic inputs in the generation of the depolarizing plateau upon which individual spindle waves develop in RE cells. (a) The components of this depolarizing plateau behave as postsynaptic excitatory events when neurons are hyperpolarized to −75 mV. (b) The amplitude of the depolarizing plateau is related to the presumed degree of synchronization in the network. Indeed, during spontaneous waxing-and-waning spindle sequences (such as under barbiturate anaesthesia) the depolarizing plateau slowly rises and falls, whereas during evoked spindles the depolarizing plateau reaches its maximum from the onset (Fig. 8). (c) With hyperpolarization at V_m levels more negative than −75 mV, the decreased amplitude of the depolarizing plateau and of the associated phasic events may be explained by the activation of inward rectification in RE cells that are able to reduce their input resistance by up to 50% (Contreras *et al.* 1993). It should also be emphasized that the constant frequency of spindles within a broad range of V_m values is indicative for the overwhelming of intrinsic oscillatory properties of RE cells (Mulle *et al.* 1986; Avanzini *et al.* 1989; Bal & McCormick, 1993) by network operations during spindles.

The depolarizing plateau seen *in vivo* is absent in perigeniculate RE cells recorded from ferret slices, a condition under which RE cells undergo a progressive hyperpolarization (von Krosigk, Bal & McCormick, 1993; Bal, von Krosigk & McCormick, 1995*b*). This difference may be explained by several network factors, including the actions of some brainstem neuromodulatory systems as well as corticothalamic inputs that are absent in the slice. The claim might also be made that the depolarizing plateau observed *in vivo* is due to a lower membrane input resistance of RE neurons, as a consequence of the impalement. That the latter explanation is not valid is demonstrated by the pattern of extracellularly recorded discharges during natural sleep, when RE neurons fire rhythmic spike bursts followed by a prolonged tonic tail of action potentials, extending throughout the duration of a spindle sequence (see Fig. 5A2 in Steriade *et al.* 1986). This aspect, seen in an extracellular position that precludes a compromised integrity of membrane input resistance, is indicative for the depolarization of RE cells during spindle sequences. The same pattern was described in the present experiments in which the depolarizing envelope of RE cells associated with a tail of tonic single-spike discharges was only seen at a relatively depolarized V_m (Fig. 9*B*), as is probably the case in the behaving animal in which neuromodulatory systems and corticothalamic projections are intact. The tonic discharges of RE cells after spindle waves may explain the tail hyperpolarization, associated with an increased conductance, in TC neurons after the completion of a spindle sequence *in vivo* (see Fig. 8 in Nuñez, Curró Dossi, Contreras & Steriade, 1992).

An important requirement for triggering of spike bursts by TC cells following their rhythmic IPSPs during spindle oscillation is an adequate V_m. Our results show that slight hyperpolarizations of TC cells, which may otherwise be silent during spindling (Fig. 13*A*; see also Nuñez *et al.* 1992), bring the IPSPs into the range of LTS deinactivation and thus, spike bursts are triggered when the V_m returns to resting values (Fig. 13*B*).

Corticothalamic feedback during spindling

Our results suggest a multiple role for the corticothalamic input during spindle oscillations.

(a) Cortical inputs proved much more efficient for eliciting spindle sequences in extra- and intracellularly recorded TC cells than stimulation of prethalamic pathways (Steriade *et al.* 1972, 1990). Moreover, during the cortically generated slow sleep oscillation, inputs from antidromically identified corticothalamic neurons trigger and pace spindle sequences in thalamic neurons with a frequency lower than 1 Hz (see Fig. 5 in Steriade *et al.* 1993*c*). Under ketamine–xylazine anaesthesia, sequences of spindle waves recur with a higher frequency, 0·6–0·9 Hz, than under urethane anaesthesia, 0·3–0·6 Hz (Steriade *et al.* 1993*b*). Under barbiturate anaesthesia and in thalamic slices, when the cortical slow rhythm is not present, spindle sequences recur with a rhythm of 0·1–0·2 Hz (Steriade & Deschênes, 1984, 1988; von Krosigk *et al.* 1993; Bal *et al.* 1995*a*, *b*) whose origin is not yet determined, but that does not depend on the cortex as it also appears in the isolated RE nucleus (Steriade *et al.* 1987).

(b) Spindle sequences could be synchronized among the two hemispheres from the outset (Fig. 12). This phenomenon can hardly be explained by ascribing to the cortex the role of a passive receiver of TC spike bursts at the spindle frequency. Rather, what probably underlies the simultaneity of spindle sequences between the two hemispheres is a wide intracortical synchronization of the slow oscillation (Amzica & Steriade, 1995), coupled with the power of corticothalamic drives to elicit spindle sequences. The reticulo-reticular thalamic commissural pathways (Battaglia, Lizier, Colacitti, Princivalle & Spreafico, 1994) should also be taken in consideration among the possible factors accounting for the synchronization of spindles between the two hemispheres.

(c) Cortical stimulation proved quite efficient to increase the synchrony between RE neurons (Fig. 10). Synchronized volleys of cortical origin trigger an EPSP followed by long-lasting hyperpolarizations in RE cells (Contreras & Steriade, 1995) from which they are released in phase and originate synchronized spindle sequences.

Concluding remarks on spindle generation

Sleep spindles appear when cortical and brainstem neurons, with activating actions on thalamic neurons, have already begun to slow down their discharge frequencies (see Steriade & McCarley, 1990). The decreased release of excitatory neurotransmitters leads to progressive hyperpolarizations that may be followed by rebound spike bursts in thalamic neurons. These events are hallmark electrophysiological signs during the behavioural state of resting sleep. Similar disfacilitation processes, leading to rhythmic spike bursts within the frequency range of spindles, occur in a subset of corticothalamic neurons (Steriade, 1978) and are probably due to the diminished firing rates of afferent basal forebrain cholinergic and monoamine-containing neurons. The hyperpolarizations and spike bursts that appear in thalamic and cortical cells with transition from waking to sleep are decisive factors to the development of synchronized spindle oscillations. In thalamic slices, spindles may be initiated by spike bursts in thalamic reticular cells, imposing IPSPs that de-inactivate rebound bursts in target-relay cells, followed by synaptic excitation of reticular neurons, with progressive recruitment of neurons in the network (Bal *et al.* 1995*b*), as similarly envisioned by Andersen & Andersson (1968) within the conceptual framework of a hypothetical intranuclear recurrent inhibitory circuit. In brain-intact animals, the diminished activity in afferent cortical, brainstem, and hypothalamic neurons achieves the incipient conditions towards the hyperpolarizations and spike bursts of reticular and cortical-projecting thalamic cells (Steriade *et al.* 1987), but the synchronization of spindles throughout thalamocortical systems is greatly potentiated by corticothalamic volleys, as generated periodically during the slow oscillation. Although the thalamic reticular nucleus can generate spindles in clustered neuronal pools or some of its sectors, even after complete disconnection, modelling studies show that the full synchronization of this nucleus and, by consequence, of thalamocortical systems, is helped by extrinsic excitatory projections (Destexhe, Contreras, Sejnowski & Steriade, 1994*a*; Golomb, Wang & Rinzel, 1994). The present data show that among the afferent excitatory inputs, the cortex plays a very potent role. The presence of modulatory systems, including the corticothalamic projection, may also explain, at least partially, the difference between the presence of spindles in the isolated rostral pole of reticular nucleus *in vivo* (Steriade *et al.* 1987) and the absence of this oscillation in perigeniculate reticular cells *in vitro* (von Krosigk *et al.* 1993). Indeed, a recent study (Destexhe, Contreras, Sejnowski & Steriade, 1994*b*) introduced the actions of depolarizing neuromodulators in model thalamic reticular neurons organized with dense proximal connectivity, and demonstrated that waxing-and-waning spindles appear at a level of membrane polarization that would correspond to a weak activity in activating systems, as is the case under anaesthesia or sleep, but are absent at more hyperpolarized levels, as may be the case in slices. Thus, the scenario of spindling generation is quite complex *in vivo* when the thalamus is embedded in networks that include the cerebral cortex and a series of neuromodulatory brainstem and hypothalamic systems.

Amzica, F. & Steriade, M. (1995). Short- and long-range neuronal synchronization of the slow (< 1 Hz) cortical oscillation. *Journal of Neurophysiology* **73**, 20–38.

Andersen, P. & Andersson, S. (1968). *Physiological Basis of the Alpha Rhythm.* Appleton-Century-Crofts, New York.

Avanzini, G., de Curtis, M., Panzica, F. & Spreafico, R. (1989). Intrinsic properties of nucleus reticularis thalami neurones of the rat studied *in vitro*. *Journal of Physiology* **416**, 111–122.

Avoli, M., Gloor, P., Kostopoulos, G. & Gotman, J. (1983). An analysis of penicillin-induced spike and wave discharges using simultaneous recordings of cortical and thalamic neurons. *Journal of Neurophysiology* **50**, 819–837.

Bal, T. & McCormick, D. A. (1993). Mechanisms of oscillatory activity in guinea-pig nucleus reticularis thalami *in vitro*: a mammalian pacemaker. *Journal of Physiology* **468**, 669–691.

Bal, T., von Krosigk, M. & McCormick, D. A. (1995*a*). Synaptic and membrane mechanisms underlying synchronized oscillations in the ferret lateral geniculate nucleus *in vitro*. *Journal of Physiology* **483**, 641–663.

Bal, T., von Krosigk, M. & McCormick, D. A. (1995*b*). Role of the ferret perigeniculate nucleus in the generation of synchronized oscillations *in vitro*. *Journal of Physiology* **483**, 665–685.

Battaglia, G., Lizier, C., Colacitti, C., Princivalle, A. & Spreafico, R. (1994). Reticuloreticular commissural pathway in the rat thalamus. *Journal of Comparative Neurology* **347**, 127–138.

Connors, B. W., Malenka, R. C. & Silva, L. R. (1988). Two inhibitory postsynaptic potentials, and $GABA_A$ and $GABA_B$ receptor-mediated responses in neocortex of rat and cat. *Journal of Physiology* **406**, 443–468.

Contreras, D., Curró Dossi, R. & Steriade, M. (1993). Electrophysiological properties of cat reticular thalamic neurons *in vivo*. *Journal of Physiology* **470**, 273–294.

Contreras, D. & Steriade, M. (1995). Cellular basis of EEG slow rhythms: a study of dynamic corticothalamic relationships. *Journal of Neuroscience* **15**, 604–622.

Crunelli, V., Haby, M., Jassik-Gerschenfeld, D., Leresche, N. & Pirchio, M. (1988). Cl^-- and K^+-dependent inhibitory postsynaptic potentials evoked by interneurones of the rat lateral geniculate nucleus. *Journal of Physiology* **399**, 153–176.

Destexhe, A., Contreras, D., Sejnowski, T. J. & Steriade, M. (1994*a*). A model of spindle rhythmicity in the isolated thalamic reticular nucleus. *Journal of Neurophysiology* **72**, 803–818.

Destexhe, A., Contreras, D., Sejnowski, T. J. & Steriade, M. (1994*b*). Modeling the control of reticular thalamic oscillations by neuromodulators. *Neuroreport* **5**, 2217–2220.

Domich, L., Oakson, G. & Steriade, M. (1986). Thalamic burst patterns in the naturally sleeping cat: a comparison between cortically projecting and reticularis neurones. *Journal of Physiology* **379**, 429–450.

Golomb, D., Wang, X.-J. & Rinzel, J. (1994). Synchronization properties of spindle oscillations in a thalamic reticular model. *Journal of Neurophysiology* **72**, 1109–1126.

HUGUENARD, J. R. & PRINCE, D. A. (1992). A novel T-type current underlies prolonged Ca^{2+}-dependent burst firing in GABAergic neurons of rat thalamic reticular nucleus. *Journal of Neuroscience* **12**, 3804–3817.

HUGUENARD, J. R. & PRINCE, D. A. (1994). Intrathalamic rhythmicity studied *in vitro*: nominal T current modulation causes robust anti-oscillatory effects. *Journal of Neuroscience* **14**, 5485–5502.

LLINÁS, R. R. & JAHNSEN, H. (1982). Electrophysiology of mammalian neurones *in vitro*. *Nature* **297**, 406–408.

MCCORMICK, D. A. & PAPE, H.-C. (1990). Properties of a hyperpolarization-activated cation current and its role in rhythmic oscillation in thalamic relay neurones. *Journal of Physiology* **431**, 291–318.

MORISON, R. S. & BASSETT, D. L. (1945). Electrical activity of the thalamus and basal ganglia in decorticated cats. *Journal of Neurophysiology* **8**, 309–314.

MULLE, C., MADARIAGA, A. & DESCHÊNES, M. (1986). Morphology and electrophysiological properties of reticularis thalami neurons in cat: *in vivo* study of a thalamic pacemaker. *Journal of Neuroscience* **6**, 2134–2145.

NUÑEZ, A., CURRÓ DOSSI, R., CONTRERAS, D. & STERIADE, M. (1992). Intracellular evidence for incompatibility between spindle and delta oscillations in thalamocortical neurons of cat. *Neuroscience* **48**, 75–85.

STERIADE, M. (1978). Cortical long-axoned cells and putative interneurons. *Behavioral and Brain Sciences* **3**, 465–514.

STERIADE, M. & AMZICA, F. (1994). Dynamic coupling among neocortical neurons during evoked and spontaneous spike-wave seizure activity. *Journal of Neurophysiology* **72**, 2051–2069.

STERIADE, M. & CONTRERAS, D. (1995). Relations between cortical and thalamic cellular events during transition from sleep patterns to paroxysmal activity. *Journal of Neuroscience* **15**, 623–642.

STERIADE, M., CONTRERAS, D., CURRÓ DOSSI, R. & NUÑEZ, A. (1993*a*). The slow (< 1 Hz) oscillation in reticular thalamic and thalamocortical neurons: scenario of sleep rhythm generation in interacting thalamic and neocortical networks. *Journal of Neuroscience* **13**, 3284–3299.

STERIADE, M. & DESCHÊNES, M. (1984). The thalamus as a neuronal oscillator. *Brain Research Reviews* **8**, 1–63.

STERIADE, M. & DESCHÊNES, M. (1988). Intrathalamic and brainstem-thalamic networks involved in resting and alert states. In *Cellular Thalamic Mechanisms*, ed. BENTIVOGLIO, M. & SPREAFICO, R., pp. 51–76. Elsevier, Amsterdam.

STERIADE, M., DESCHÊNES, M., DOMICH, L. & MULLE, C. (1985). Abolition of spindle oscillations in thalamic neurons disconnected from nucleus reticularis thalami. *Journal of Neurophysiology* **54**, 1473–1497.

STERIADE, M., DOMICH, L. & OAKSON, G. (1986). Reticularis thalamic neurons revisited: activity changes during shifts in states of vigilance. *Journal of Neuroscience* **6**, 68–81.

STERIADE, M., DOMICH, L., OAKSON, G. & DESCHÊNES, M. (1987). The deafferented reticularis thalami nucleus generates spindle rhythmicity. *Journal of Neurophysiology* **57**, 260–273.

STERIADE, M., JONES, E. G. & LLINÁS, R. R. (1990). *Thalamic Oscillations and Signaling*. John Wiley and Sons, New York.

STERIADE, M. & MCCARLEY, R. W. (1990). *Brainstem Control of Wakefulness and Sleep*. Plenum, New York.

STERIADE, M., NUÑEZ, A. & AMZICA, F. (1993*b*). A novel slow (< 1 Hz) oscillation of neocortical neurones *in vivo*: depolarizing and hyperpolarizing components. *Journal of Neuroscience* **13**, 3252–3265.

STERIADE, M., NUÑEZ, A. & AMZICA, F. (1993*c*). Intracellular analysis of relations between the slow (< 1 Hz) neocortical oscillation and other sleep rhythms of the electroencephalogram. *Journal of Neuroscience* **13**, 3266–3283.

STERIADE, M., WYZINSKI, P. & APOSTOL, V. (1972). Corticofugal projections governing rhythmic thalamic activity. In *Corticothalamic Projections and Sensorimotor Activities*, ed. FRIGYESI, T. L., RINVIK, E. & YAHR, M. D., pp. 221–272. Raven Press, New York.

VON KROSIGK, M., BAL, T. & MCCORMICK, D. A. (1993). Cellular mechanisms of a synchronized oscillation in the thalamus. *Science* **261**, 361–364.

YEN, C. T. & JONES, E. G. (1983). Intracellular staining of physiologically identified neurons and axons in the somatosensory thalamus of the cat. *Brain Research* **280**, 148–154.

Acknowledgements

This work was supported by the Medical Research Council of Canada (grant MT-3689). D.C. is a PhD student and is partially supported by a fellowship from the Savoy Foundation. We thank P. Giguère and D. Drolet for technical assistance.

Received 17 January 1995; accepted 6 July 1995.